

Templated Formation of Binuclear Macrocycles via Hemilabile Ligands

Joshua R. Farrell,[†] Adam H. Eisenberg,[†] Chad A. Mirkin,^{*,†} Ilia A. Guzei,[‡]
Louise M. Liable-Sands,[‡] Christopher D. Incarvito,[‡] Arnold L. Rheingold,[‡] and
Charlotte L. Stern[†]

Department of Chemistry, 2145 Sheridan Road, Northwestern University,
Evanston, Illinois 60208, and Department of Chemistry and Biochemistry,
University of Delaware, Newark, Delaware 19716

Received July 26, 1999

A new approach to synthesizing binuclear metallomacrocycles is reported. This approach utilizes flexible bisphosphine alkyl–aryl ether hemilabile ligands which complex Rh(I) to form “condensed” macrocycles held together by a series of both strong and weak links of the following type: $[(\kappa^2:\mu^2:\kappa^2-(1,4-(\text{Ph}_2\text{PCH}_2\text{CH}_2\text{O})_2-2,3,5,6-((\text{CH}_3)_4\text{C}_6))_2\text{Rh}_2][\text{BF}_4]_2$ (**5a**) or $[(\mu^2,\eta^1:\eta^6:\eta^1-(1,4-(\text{Ph}_2\text{P}(\text{CH}_2)_n\text{O})_2\text{X})_2\text{Rh}_2][\text{BF}_4]_2$ (**5b**, $n = 2$, $\text{X} = 2,3,5,6-((\text{CH}_3)_4\text{C}_6)$; **6**, $n = 3$, $\text{X} = 2,3,5,6-((\text{CH}_3)_4\text{C}_6)$; **7**, $n = 2$, $\text{X} = \text{C}_6\text{H}_4$; **8**, $n = 2$, $\text{X} = \text{C}_6\text{H}_4-\text{C}_6\text{H}_4$). Introduction of ligands that will bind to Rh(I) more strongly than either the Rh– η^6 -aryl or Rh– η^1 -ether weak links of **5a–8** results in the breaking of the weak links to form a series of 26–34-membered macrocyclic ring structures such as $[(\mu^2-(1,4-(\text{Ph}_2\text{P}(\text{CH}_2)_n\text{O})_2\text{X})_2(\text{L}_1)_m(\text{L}_2)_o\text{Rh}_2][\text{BF}_4]_2$ (**9**, $n = 2$, $\text{X} = 2,3,5,6-((\text{CH}_3)_4\text{C}_6)$, $\text{L}_1 = \text{CO}$, $m = 6$, $\text{L}_2 = \text{none}$; **10**, $n = 2$, $\text{X} = \text{C}_6\text{H}_4$, $\text{L}_1 = \text{CO}$, $m = 6$, $\text{L}_2 = \text{none}$; **11**, $n = 2$, $\text{X} = \text{C}_6\text{H}_4-\text{C}_6\text{H}_4$, $\text{L}_1 = \text{CO}$, $m = 6$, $\text{L}_2 = \text{none}$; **12**, $n = 2$, $\text{X} = 2,3,5,6-((\text{CH}_3)_4\text{C}_6)$, $\text{L}_1 = \text{CO}$, $m = 2$, $\text{L}_2 = \text{CH}_3\text{CN}$, $o = 2$; **13**, $n = 3$, $\text{X} = 2,3,5,6-((\text{CH}_3)_4\text{C}_6)$, $\text{L}_1 = \text{CO}$, $m = 2$, $\text{L}_2 = \text{CH}_3\text{CN}$, $o = 2$; **14**, $n = 2$, $\text{X} = \text{C}_6\text{H}_4$, $\text{L}_1 = \text{CO}$, $m = 2$, $\text{L}_2 = \text{CH}_3\text{CN}$, $o = 2$; **15**, $n = 2$, $\text{X} = \text{C}_6\text{H}_4-\text{C}_6\text{H}_4$, $\text{L}_1 = \text{CO}$, $m = 2$, $\text{L}_2 = \text{CH}_3\text{CN}$, $o = 2$). These homobimetallic macrocycles can be used to sequester bifunctional aromatic molecules to form host–guest structures such as $[(\mu^2-(1,4-(\text{Ph}_2\text{PCH}_2\text{CH}_2\text{O})_2-2,3,5,6-((\text{CH}_3)_4\text{C}_6))_2(\text{CO})_2(\mu^2-1,4-(\text{NC})_2\text{C}_6\text{H}_4)-\text{Rh}_2][\text{BF}_4]_2$ (**16**) and $[(\mu^2-(1,4-(\text{Ph}_2\text{PCH}_2\text{CH}_2\text{O})_2-2,3,5,6-((\text{CH}_3)_4\text{C}_6))_2(\text{CH}_3\text{CN})_2(\mu^2-1,4-(\text{CN})_2\text{C}_6\text{H}_4)-\text{Rh}_2][\text{BF}_4]_2$ (**17**). The synthetic methods described within this article represent a powerful new way of making binuclear macrocycles from flexible ligands in nearly quantitative yields. Moreover, the macrocycles are highly tailorable with respect to cavity size and hydrophobicity and the metals’ steric and electronic environments. Solid-state structures as determined by single-crystal X-ray diffraction studies are presented for compounds **5a**, **6**, **7**, **9**, **10**, **12**, and **17**.

Introduction

Metallomacrocycles comprise an extremely active area of research that is important for the development of host–guest chemistry, catalysis, receptor site design, and even molecular electronics.^{1–4} Several elegant synthetic methods have been developed that allow one to prepare complex structures with tailorable properties, sometimes even in exceptionally high yields. Using these methods, various groups have designed macrocycles incorporating a diverse variety of metals and ligands.^{1–3,5–25} However, there are often significant

limitations associated with some of these synthetic methods, which prohibit their generality with respect to either transition metal or bridging ligand.

* To whom correspondence should be addressed. Fax: (847) 491-7713. E-mail: camirkin@chem.nwu.edu.

[†] Northwestern University.

[‡] University of Delaware.

(1) Lehn, J.-M. *Supramolecular Chemistry*; VCH: New York, 1995.

(2) Lehn, J.-M. *Science* **1993**, *260*, 1762–1763.

(3) Vögtle, F. *Supramolecular Chemistry*; Wiley: Chichester, 1991.

(4) Mirkin, C. A.; Ratner, M. A. *Annu. Rev. Phys. Chem.* **1992**, *43*, 719–754.

(5) Lindner, E.; Hermann, C.; Baum, G.; Fenske, D. *Eur. J. Inorg. Chem.* **1999**, 679–685.

(6) Müller, C.; Whiteford, J. A.; Stang, P. J. *J. Am. Chem. Soc.* **1998**, *120*, 9827–9837.

(7) Ibukuro, F.; Kusakawa, T.; Fujita, M. *J. Am. Chem. Soc.* **1998**, *120*, 8561–8562.

(8) Woessner, S. M.; Helms, J. B.; Shen, Y.; Sullivan, B. P. *Inorg. Chem.* **1998**, *31*, 5406–5407.

(9) Benkstein, K. D.; Hupp, J. T.; Stern, C. L. *Inorg. Chem.* **1998**, *37*, 5404–5405.

(10) Bassani, D. M.; Lehn, J.-M.; Fromm, K.; Fenske, D. *Angew. Chem., Int. Ed.* **1998**, *37*, 2364–2367.

(11) Hanan, G. S.; Volkmer, D.; Schubert, U. S.; Lehn, J.-M.; Baum, G.; Fenske, D. *Angew. Chem., Int. Ed. Engl.* **1997**, *36*, 1842–1844.

(12) Stang, P. J. *Chem. Eur. J.* **1998**, *4*, 19–27.

(13) Olenyuk, B.; Fechtenkötter, A.; Stang, P. J. *J. Chem. Soc., Dalton Trans.* **1998**, 1707–1728.

(14) Stang, P. J.; Olenyuk, B. *Acc. Chem. Res.* **1997**, *30*, 502–518.

(15) Hartshorn, C. M.; Steel, P. J. *Chem. Commun.* **1997**, 541–542.

(16) Fujita, M.; Sasaki, O.; Mituhashi, T.; Fujita, T.; Yazaki, J.; Yamaguchi, K.; Ogura, K. *Chem. Commun.* **1996**, 1535–1536.

(17) Fujita, M.; Ogura, K. *Coord. Chem. Rev.* **1996**, *148*, 249–264.

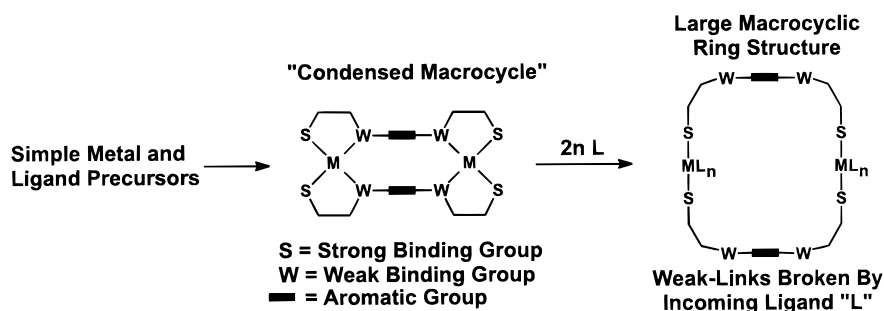
(18) Baxter, P. N. W.; Hanan, G. S.; Lehn, J.-M. *Chem. Commun.* **1996**, 2019–2020.

(19) Fujita, M.; Ibukuro, F.; Yamaguchi, K.; Ogura, K. *J. Am. Chem. Soc.* **1995**, *117*, 4175–4176.

(20) Fujita, M.; Oguro, D.; Mlyazawa, M.; Oka, H.; Yamaguchi, K.; Ogura, K. *Nature* **1995**, *378*, 469–471.

(21) Fujita, M.; Yazaki, J.; Ogura, K. *J. Am. Chem. Soc.* **1990**, *112*, 5645–5647.

Scheme 1



When designing a synthetic route to a large macrocyclic structure, entropic effects are a major consideration. Competitive pathways involving the formation of oligomers and polymers often dominate and reduce the obtained yields of target macrocyclic structures.²⁶ One method for combating this problem is the use of rigid ligands combined with metal centers with available adjacent, often *cis*, coordination sites which drive the formation of a closed triangular, square, rectangle, or hexagon-like structure. Although the use of rigid ligands and metals with adjacent coordination sites offers the advantage that one can synthesize such complex structures, the use of such ligands does pose a significant limitation with regard to the types of macrocyclic structures that can be targeted. Moreover, the "square approach" typically results in the formation of transition metal complexes that are coordinatively saturated and often substitutionally inert.¹³ To fully realize the potential of metallomacrocycles, new general complementary synthetic routes that allow use of structurally flexible ligands and do not saturate the coordination spheres of transition metals need to be developed. Note that there are some examples of coordinatively saturated multimetallic macrocycles generated from flexible ligands, but there are essentially no high-yield, general synthetic methods for such systems.^{27–29}

Herein, we report a novel, one-pot,³⁰ high-yield approach to the synthesis of binuclear macrocycles from structurally flexible hemilabile phosphino aryl-ether ligands.²⁴ This strategy minimizes the entropic cost of using a flexible ligand to prepare a macrocyclic structure by first forming a "condensed" structure stabilized by a series of weak links and π - π interactions (Scheme 1). The weak links in the condensed structures can then be broken with more strongly ligating ligands, causing them to open into large binuclear ring structures (Scheme 1). Furthermore, the reactivity and coordina-

tive unsaturation of the metal centers in these macrocycles allow for the sequestration of bifunctional aromatic molecules leading to host-guest structures (*vide infra*). Because of the generality and versatility of this synthetic method, this approach should be particularly appealing to those interested in receptor-site design and shape-selective catalysis. The purpose of this article is to demonstrate that the "weak-link" approach to macrocycle synthesis is broadly applicable to the preparation of structures with tailorable properties. In particular, we show that macrocycle size, pocket hydrophobicity, and both the steric and electronic environments of the metal centers holding the macrocycle together can be controlled through judicious choice of ligands and conditions. Finally, we have investigated a number of factors that control the formation of these unusual structures which provide important insight into how and why these structures form, as well as the scope of this synthetic strategy. A preliminary report of this work has appeared in the literature.²⁴

Experimental Section

General Procedures. Unless otherwise noted, all reactions were carried out under a nitrogen atmosphere using standard Schlenk techniques. Diethyl ether and tetrahydrofuran were dried and distilled over sodium benzophenone. Acetonitrile, methylene chloride, and pentane were dried and distilled over calcium hydride. $[\text{Rh}(\mu\text{-Cl})(\text{COE})_2]_x$ ³¹ (COE = cyclooctene) and dihydroxy durene³² were prepared according to literature methods. All other chemicals were obtained from commercial sources and used as received unless otherwise noted.

Physical Measurements. NMR spectra were recorded on a Varian Gemini 300 MHz or Varian Unity 400 MHz FT-NMR spectrometer. ¹H NMR signals are reported relative to residual proton resonances in deuterated solvents. ³¹P{¹H} chemical shifts were measured relative to an external 85% H₃PO₄ standard. ¹⁹F{¹H} NMR spectra were measured relative to an external CFCl₃ standard. ¹³C NMR spectra for the metal complexes have not been reported because of their low solubilities. ¹H NOE difference spectroscopy was performed on a Varian Unity 400 MHz FT-NMR spectrometer. Elemental analyses were done by Desert Analytics, Tucson, AZ. Fast atom bombardment (FAB) and electron ionization (EI) mass spectra were recorded on a Fisons VG 70-250 SE mass spectrometer. Electrospray (ES) mass spectra were recorded on a Micromass Quatro II electrospray triple quadrupole mass spectrometer. IR spectra were recorded on a Nicolet 520 FT-IR spectrometer. Melting points were recorded on a Mel-Temp II melting temperature apparatus made by Laboratory Devices of Holliston, MA.

(22) Stricklen, P. M.; Volcko, E. J.; Verkade, J. G. *J. Am. Chem. Soc.* **1983**, *105*, 2494–2495.

(23) (a) Farrell, J. R.; Mirkin, C. A.; Liable-Sands, L. M.; Rheingold, A. L. *J. Am. Chem. Soc.* **1998**, *120*, 11834–11835. (b) Holliday, B. J.; Farrell, J. R.; Mirkin, C. A.; Lam, K.-C.; Rheingold, A. L. *J. Am. Chem. Soc.* **1999**, *121*, 6316–6317.

(24) Farrell, J. R.; Mirkin, C. A.; Guzei, I. A.; Liable-Sands, L. M.; Rheingold, A. L. *Angew. Chem., Int. Ed.* **1998**, *37*, 465–467.

(25) Caulder, D. L.; Raymond, K. N. *J. Chem. Soc., Dalton Trans.* **1999**, *8*, 1185–1200.

(26) Sanders, J. K. M. *Chem. Eur. J.* **1998**, *4*, 1378–1383.

(27) Fujita, M.; Nagao, S.; Iida, M.; Ogata, K.; Ogura, K. *J. Am. Chem. Soc.* **1993**, *115*, 1574–1576.

(28) March, F. C.; Mason, R.; Thomas, K. M.; Shaw, B. L. *J. Chem. Soc., Chem. Commun.* **1975**, 584–585.

(29) Sanger, A. R. *J. Chem. Soc., Chem. Commun.* **1975**, 893–894.

(30) A "one-pot" reaction implies that a reaction, including one or more steps, occurs in a single flask without isolation or characterization of intermediates.

(31) Ent, A.; Onderdelinden, A. L. In *Reagents for Transition Metal Complex and Organometallic Syntheses*; Angelici, R. J., Ed.; John Wiley & Sons: New York, 1990; Vol. 28, pp 90–91.

(32) Thomas, A. D.; Miller, L. L. *J. Org. Chem.* **1986**, *51*, 4160–4169.

Synthesis of 1,4-(–OCH₂CH₂Cl)₂-2,3,5,6-((CH₃)₄C₆) (1a). Dihydroxydurene (0.25 g, 1.5 mmol), KOH (0.68 g, 12.1 mmol), 2-chloroethyl *p*-toluenesulfonate (1.5 g, 6.04 mmol), the phase transfer catalyst Et₄Ni (0.0193 g, 0.075 mmol), and 30 mL of distilled water were added to a reaction vessel and refluxed for 16 h. After 16 h, the crude solution mixture was cooled and washed with 150 mL of CH₂Cl₂ in air. The organic phase was separated and dried over MgSO₄, and then, the solvent was removed by rotary evaporation. The crude product was washed with 20 mL of EtOH to remove unreacted 2-chloroethyl *p*-toluenesulfonate and filtered through Celite on a glass frit. The product was redissolved in CH₂Cl₂ and passed through the Celite. Rotary evaporation of the solvent yielded **1a** as an analytically pure, air-stable, white powder (yield = 80%, 0.349 g, 1.2 mmol). ¹H NMR: (CDCl₃) δ 3.91 (t, 4H, CH₂O, *J*_{H–H} = 5.8 Hz), 3.83 (t, 4H, CH₂Cl, *J*_{H–H} = 5.5 Hz), 2.17 (s, 12H, CH₃). MS(EI): [M]⁺ calcd = 291.2, expt = 291.2 *m/z*. Anal. Calcd for C₁₄H₂₀O₂Cl₂: C, 57.74; H, 6.92. Found: C, 57.60; H, 6.70. Mp = 128.0–128.5 °C.

Synthesis of 1,4-(–OCH₂CH₂CH₂Cl)₂-2,3,5,6-((CH₃)₄C₆) (2a). Duroquinone (2.00 g, 12 mmol), (*n*-Bu)₄NBr (0.45 g, 1.2 mmol), and NaHSO₃ (20.9 g, 120 mmol) were combined in a solution of THF/H₂O (25/15 mL) and stirred for 15 min. To this solution, KOH (15.5 g, 280 mmol) dissolved in a minimal amount of distilled H₂O was added. After 15 min, BrCH₂CH₂CH₂Cl (18.9 g, 120 mmol) was added, and the reaction mixture was refluxed for 2 h. After the reaction mixture cooled, the organic products were extracted with CH₂Cl₂ in air. The CH₂Cl₂ solution was dried with MgSO₄ and filtered, and then the solvent was removed via rotary evaporation to yield a light yellow oil. Upon standing for 2 h, white crystals of **2a** fell out of the oil. The air-stable crystals were washed with pentane to afford analytically pure **2a** (yield = 16%, 0.600 g, 1.89 mmol). ¹H NMR: (CD₂Cl₂) δ 3.85 (t, 4H, CH₂O, *J*_{H–H} = 6.5 Hz), 3.77 (t, 4H, CH₂Cl, *J*_{H–H} = 5.9 Hz), 2.23 (quintuplet, 4H, CH₂CH₂CH₂, *J*_{H–H} = 5.9 Hz), 2.15 (s, 12H, CH₃). MS(EI): [M]⁺ calcd = 318.5113, expt = 318.5110 *m/z*. Mp = 71–73 °C.

Synthesis of 1,4-(–OCH₂CH₂Cl)₂C₆H₄ (3a). Potassium carbonate (25.98 g, 0.188 mol) and 2-chloroethyl *p*-toluenesulfonate (20.6 mL, 26.6 g, 0.114 mol) were refluxed in THF under nitrogen for 1 h. A solution of hydroquinone (2.50 g, 0.0227 mol) in THF (125 mL) was slowly added to the refluxing solution over 45 min. The reaction mixture was then refluxed for 7 days. After cooling, the mixture was filtered, the solvent was removed in vacuo, and the product was extracted with CH₂Cl₂ from an aqueous solution made slightly acidic with 1 M HCl in air. The solvent was removed by rotary evaporation to yield a tan solid. Column chromatography of the crude product on silica gel with toluene as the eluent produced two bands. The first band contained pure product, and the second band contained unreacted 2-chloroethyl *p*-toluenesulfonate. The solvent was removed in vacuo to yield pure **3a** as an air-stable, white powder (yield = 58%, 3.102 g, 13.2 mmol). ¹H NMR: (CDCl₃) δ 6.88 (s, 4H, C₆H₄), 4.20 (t, 4H, CH₂O, *J*_{H–H} = 5.9 Hz), 3.01 (t, 4H, CH₂Cl, *J*_{H–H} = 5.9 Hz). MS(EI): [M]⁺ calcd = 234.02144, expt = 234.02144 *m/z*. Mp = 96.8–97.2 °C.

Synthesis of 4,4'-(–OCH₂CH₂Cl)₂-C₆H₄-C₆H₄ (4a). 4,4'-Biphenol (1.00 g, 5.37 mmol), KOH (2.41 g, 43.0 mmol), 2-chloroethyl *p*-toluenesulfonate (6.30 g, 29.9 mmol), and Et₄Ni (0.069 g, 0.27 mmol) were reacted in a fashion analogous to the preparation method for **1a**. Rotary evaporation yielded **4a** as an analytically pure, air-stable, white powder (yield = 43%, 0.700 g, 2.25 mmol). ¹H NMR: (CDCl₃) δ 7.50 (d, 4H, C₆H₄, *J*_{H–H} = 8.9 Hz), 6.97 (d, 4H, C₆H₄, *J*_{H–H} = 8.8 Hz), 4.27 (t, 4H, CH₂O, *J*_{H–H} = 5.9 Hz), 3.85 (t, 4H, CH₂Cl, *J*_{H–H} = 5.9 Hz). MS(EI): [M]⁺ calcd = 310.0527, expt = 310.0523 *m/z*. Mp = 165.5–167 °C.

General Procedure for the Synthesis of 1,4-(PPh₂CH₂CH₂O)₂-2,3,5,6-((CH₃)₄C₆) (1b), 1,4-(PPh₂CH₂CH₂CH₂O)₂-2,3,5,6-((CH₃)₄C₆) (2b), 1,4-(PPh₂CH₂CH₂O)₂C₆H₄ (3b), and

4,4'-(PPh₂CH₂CH₂O)₂-C₆H₄-C₆H₄ (4b). A THF solution of KPPPh₂ (0.5 M, 5.4 mL, 2.7 mmol) was diluted with 20 mL of THF. A precursor (1.3 mmol), **1a–4a**, in 15 mL of THF was slowly added to this solution at 0 °C. The reaction was allowed to warm overnight to room temperature, and then, the solvent was removed in vacuo. The crude product was washed with 20 mL of degassed EtOH and filtered through Celite on a glass frit. The product was redissolved in CH₂Cl₂ and passed through the Celite. The solvent was removed in vacuo, and residual KCl was removed by column chromatography using a short (5 × 6 cm) column of silica gel with CH₂Cl₂ as the eluent. Removal of the solvent afforded analytically pure **1b–4b** as white powders.

1,4-(PPh₂CH₂CH₂O)₂-2,3,5,6-((CH₃)₄C₆) (1b). Yield = 91%. ¹H NMR: (CD₂Cl₂) δ 7.46 (m, 8H, P(C₆H₅)₂), 7.34 (m, 12H, P(C₆H₅)₂), 3.71 (m, 4H, CH₂O, *J*_{H–H} = 6.3 Hz), 2.60 (t, 4H, CH₂P, *J*_{H–H} = 7.9 Hz), 2.04 (s, 12H, CH₃). ³¹P{¹H} NMR: (CD₂Cl₂) δ –22.4 (s). MS(EI): [M]⁺ calcd = 590.2504, expt = 590.2504 *m/z*; mp = 157–158.5 °C.

1,4-(PPh₂CH₂CH₂O)₂-2,3,5,6-((CH₃)₄C₆) (2b). Yield = 60%. ¹H NMR: (CD₂Cl₂) δ 7.46 (m, 8H, P(C₆H₅)₂), 7.34 (m, 12H, P(C₆H₅)₂), 3.70 (t, 4H, CH₂O, *J*_{H–H} = 6.3 Hz), 2.27 (b, 4H, CH₂P), 2.11 (s, 12H, CH₃), 1.90 (b, 4H, CH₂CH₂CH₂). ³¹P{¹H} NMR: (CD₂Cl₂) δ –15.6 (s). MS(EI): [M – H]⁺ calcd = 619.2889, expt = 619.2881 *m/z*. Mp = 122.0–123.5 °C.

1,4-(PPh₂CH₂CH₂O)₂C₆H₄ (3b). Yield = 74%. ¹H NMR: (CDCl₃) δ 7.48 (m, 8H, P(C₆H₅)₂), 7.34 (m, 12H, P(C₆H₅)₂), 6.68 (s, 4H, C₆H₄), 4.04 (m, 4H, CH₂O), 2.56 (t, 4H, CH₂P, *J*_{H–H} = 7.6 Hz). ³¹P{¹H} NMR: (CDCl₃) δ –21.9 (s). MS(EI): [M – H]⁺ calcd = 533.1799, expt = 533.1795 *m/z*. Mp = 109.0–110.0 °C.

4,4'-(PPh₂CH₂CH₂O)₂-C₆H₄-C₆H₄ (4b). Yield = 77%. ¹H NMR: (CD₂Cl₂) δ 7.51–7.34 (b, 24H, C₆H₄ and P(C₆H₅)₂), 6.83 (d, 4H, C₆H₄, *J*_{H–H} = 8.9 Hz), 4.13 (m, 4H, CH₂O), 2.59 (t, 4H, CH₂P, *J*_{H–H} = 7.5 Hz). ³¹P{¹H} NMR: (CD₂Cl₂) δ –21.0 (s). MS(EI): [M – H]⁺ calcd = 609.2112, expt = 609.2115 *m/z*. Mp = 161.5–163.0 °C.

Synthesis of [(κ²:μ²:κ²-(1,4-(Ph₂PCH₂CH₂O)₂-2,3,5,6-((CH₃)₄C₆))₂Rh₂][BF₄]₂ (5a). In a glovebox [Rh(μ-Cl)(COE)₂]_x (40.0 mg, 0.111 mmol) and AgBF₄ (22 mg, 0.113 mmol) were reacted in 3 mL of CH₂Cl₂ for 1 h. The resulting reaction mixture was filtered through Celite, removing a light gray precipitate, and diluted with 125 mL of THF. To this, a solution of **1b** (66.0 mg, 0.111 mmol) in 125 mL of THF was added dropwise at –78 °C over 1 h. The solution was warmed to room temperature over 1 h followed by removal of the solvent in vacuo to yield an orange powder. This product consists of one metal–phosphorus-containing compound, **5a**, as determined by ³¹P{¹H} NMR. Washing the powder with Et₂O removed residual COE and afforded pure **5a** (yield = 90%, 0.781 g, 0.050 mmol). Recrystallization from CH₂Cl₂/Et₂O afforded orange thin blades of **5a**, which were characterized by X-ray crystallography. ¹H NMR: (CD₂Cl₂) δ 7.51 (m, 16H, P(C₆H₅)₂), 7.39 (t, 8H, P(C₆H₅)₂), 7.30 (t, 16H, P(C₆H₅)₂), 3.62 (m, 8H, CH₂O), 2.66 (m, 8H, CH₂P), 2.34 (s, 24H, CH₃). ¹⁹F NMR: (CD₂Cl₂) δ –153.0 (s, BF₄). MS(FAB⁺): [[M²⁺][BF₄][–]]⁺ calcd = 1473, expt = 1473 *m/z*.

Synthesis of [(η¹:η⁶:η¹-(1,4-(Ph₂PCH₂CH₂O)₂-2,3,5,6-((CH₃)₄C₆))Rh][BF₄] (5c). Sealing **5a** (0.010 g, 0.0064 mmol) and ClCD₂CD₂Cl (0.7 mL) in an NMR tube and heating at 75 °C for 10 days results in the conversion of **5a** to **5c** along with some minor decomposition. Slow recrystallization from CH₂Cl₂/Et₂O afforded orange prismatic crystals of **5c**, which were characterized by X-ray crystallography. ¹H NMR: (CD₂Cl₂) δ 7.0–7.4 (m, 20H, P(C₆H₅)₂), 4.05 (m, 4H, CH₂O), 2.42 (s, 12H, CH₃), 2.05 (m, 4H, CH₂P). ³¹P{¹H} NMR: (CD₂Cl₂) δ 31.2 (d, *J*_{Rh–P} = 202 Hz). MS(FAB⁺): [M]⁺ calcd = 693.2, expt = 693.2 *m/z*.

General Procedure for the Synthesis of [(μ²:η¹:η⁶:η¹-(1,4-(Ph₂PCH₂CH₂CH₂O)₂-2,3,5,6-((CH₃)₄C₆))₂Rh₂][BF₄]₂ (6), [(μ²:η¹:η⁶:η¹-(1,4-(Ph₂PCH₂CH₂O)₂C₆H₄))₂Rh₂]

[BF₄]₂ (7), and [(μ²,η¹:η⁶:η¹-(4,4'-(PPh₂CH₂CH₂O)₂-C₆H₄-C₆H₄)₂Rh₂][BF₄]₂ (8). In a glovebox, [Rh(μ-Cl(COEt)₂)₂] (40.0 mg, 0.111 mmol) and AgBF₄ (22 mg, 0.113 mmol) were reacted in 3 mL of CH₂Cl₂ for 1 h. The resulting reaction mixture was filtered through Celite to remove a light gray precipitate, which was presumably AgCl, and diluted with 125 mL of THF. To this, a 125 mL THF solution of a ligand (0.111 mmol), **2b-4b**, was added dropwise at -78 °C over 2 h. The solution was warmed to room temperature over 1 h followed by reflux for 4 h. At this elevated temperature, the solvent was removed in vacuo to yield powders in quantitative yields as determined by NMR spectroscopy. Redissolving each of the powders in CH₂Cl₂ and layering with Et₂O afforded pure **6-8**.

[(μ²,η¹:η⁶:η¹-(1,4-(Ph₂PCH₂CH₂CH₂O)₂-2,3,5,6-((CH₃)₄-C₆))₂Rh₂][BF₄]₂ (6). Recrystallization from CH₂Cl₂/Et₂O afforded red thin blades of **6**, which were characterized by X-ray crystallography. Isolated yield = 77%. ¹H NMR: (CD₂Cl₂) δ 7.11–7.40, 6.88 (m(b), 40H, P(C₆H₅)₂), 3.93 (b, 4H, CH₂O), 3.60 (b, 4H, CH₂O), 2.78 (m, 4H, CH₂P), 2.38 (m, 4H, CH₂P), 2.49 (s, 12H, CH₃), 2.27 (s, 12H, CH₃), 1.53 (b, 8H, CH₂CH₂-CH₂). MS(ES): [[M²⁺][BF₄⁻]]⁺ calcd = 1529.4, expt = 1529.6 m/z.

[(μ²,η¹:η⁶:η¹-(1,4-(Ph₂PCH₂CH₂CH₂O)₂-C₆H₄)₂Rh₂][BF₄]₂ (7). Recrystallization from CH₂Cl₂/Et₂O afforded very thin orange plates from which a X-ray crystallographic study was conducted, which provided structural and atom connectivity information. An ORTEP diagram of **7** along with important bond distances and angles and important crystallographic data can be found in the Supporting Information. After several recrystallization attempts, the best crystals that could be obtained were extremely weak and diffusely diffracting. There are two independent but chemically equivalent molecules in the asymmetric unit of **7**. Due to the crystal quality and the large number of displacement parameters, several carbon atoms of **7** could not be refined anisotropically. However, all other non-hydrogen atoms of **7** were refined with anisotropic displacement parameters. ¹H NMR: (CD₂Cl₂) δ 7.8–6.9, (m, 48H, P(C₆H₅)₂ and C₆H₄), 4.30 (m, 4H, CH₂O), 3.96 (m, 4H, CH₂O), 2.32 (m, 4H, CH₂P), 1.92 (m, 4H, CH₂P). ¹⁹F{¹H} NMR: (CD₂Cl₂) δ -151.1 (s, BF₄). MS(ES): [M]²⁺ calcd = 637.1 m/z, expt = 637.3 m/z. [[M²⁺][BF₄⁻]]⁺ calcd = 1361.2, expt = 1361.5 m/z.

[(μ²,η¹:η⁶:η¹-(4,4'-(PPh₂CH₂CH₂O)₂-C₆H₄-C₆H₄)₂Rh₂][BF₄]₂ (8). Compound **8** was isolated as an orange powder. ¹H NMR: (CD₂Cl₂) δ 7.51–7.34 (b, 24H, C₆H₄ and P(C₆H₅)₂), 6.83 (d, 4H, C₆H₄, J_{H-H} = 8.9 Hz), 4.13 (m, 4H, CH₂O), 2.59 (t, 4H, CH₂P, J_{H-H} = 7.5 Hz). MS(FAB⁺): [[M²⁺][BF₄⁻]]⁺ calcd = 1513, expt = 1513, [M]²⁺ calcd = 713, expt = 713 m/z.

General Procedure for the Synthesis of [(μ²-(1,4-(Ph₂PCH₂CH₂O)₂-2,3,5,6-((CH₃)₄C₆))₂(CO)₆Rh₂][BF₄]₂ (9), [(μ²-(1,4-(Ph₂PCH₂CH₂O)₂-C₆H₄)₂(CO)₆Rh₂][BF₄]₂ (10), and [(μ²-(4,4'-(PPh₂CH₂CH₂O)₂-C₆H₄-C₆H₄)₂(CO)₆Rh₂][BF₄]₂ (11). Complex **5a**, **7**, or **8** (0.0064 mmol) and CO (1 atm) in CD₂Cl₂ (0.7 mL) were reacted in an NMR tube for 2 h. The solution color changed from orange to yellow, indicating the formation of **9**, **10**, or **11** in a quantitative yield as determined by NMR spectroscopy.

[(μ²-(1,4-(Ph₂PCH₂CH₂O)₂-2,3,5,6-((CH₃)₄C₆))₂(CO)₆Rh₂][BF₄]₂ (9). Recrystallization from a CO-saturated solution of CH₂Cl₂/Et₂O yielded pale yellow blocks, which were characterized via a single-crystal X-ray crystallographic study. ¹H NMR: (CD₂Cl₂) δ 7.60 (m, 40H, P(C₆H₅)₂), 3.85 (m, 8H, CH₂O), 3.27 (m, 8H, CH₂P), 1.88 (s, 24H, CH₃). ³¹P{¹H} NMR: (CD₂Cl₂) δ 20 (d, J_{Rh-P} = 88 Hz).

[(μ²-(1,4-(Ph₂PCH₂CH₂O)₂-C₆H₄)₂(CO)₆Rh₂][BF₄]₂ (10). Single-crystals of **10** were grown from a supersaturated solution of CH₂Cl₂ and were characterized via X-ray crystallography. ¹H NMR: (CD₂Cl₂) δ 7.59 (m, 40H, P(C₆H₅)₂), 6.38 (s, 8H, C₆H₄), 4.29 (b, 8H, CH₂O), 3.19 (b, 8H, CH₂P). ³¹P{¹H} NMR: (CD₂Cl₂) δ 28.0 (d, J_{Rh-P} = 78 Hz).

[(μ²-(4,4'-(PPh₂CH₂CH₂O)₂-C₆H₄-C₆H₄)₂(CO)₆Rh₂][BF₄]₂ (11). ¹H NMR: (CD₂Cl₂) δ 7.61 (m, 40H, PPh₂), 7.13 (d, 8H, CH, J_{H-H} = 8.8 Hz), 6.46 (d, 8H, CH, J_{H-H} = 8.8 Hz), 4.43 (b, 8H, CH₂O), 3.26 (b, 8H, CH₂P). ³¹P{¹H} NMR: (CD₂Cl₂) δ 30.2 (d, J_{Rh-P} = 79 Hz).

General Procedure for the Synthesis of [(μ²-(1,4-(Ph₂PCH₂CH₂O)₂-2,3,5,6-((CH₃)₄C₆))₂(CO)₂(CH₃CN)₂Rh₂][BF₄]₂ (12), [(μ²-(1,4-(Ph₂PCH₂CH₂O)₂-C₆H₄)₂(CO)₂(CH₃CN)₂Rh₂][BF₄]₂ (14), and [(μ²-(4,4'-(Ph₂PCH₂CH₂O)₂-C₆H₄-C₆H₄)₂(CO)₂(CH₃CN)₂Rh₂][BF₄]₂ (15). To an NMR tube containing **9**, **10**, or **11** (6.4 μmol) in CD₂Cl₂ (0.7 mL), one drop of CH₃CN was added. The solvent was removed in vacuo, and the product was redissolved in CD₂Cl₂, yielding a yellow solution of **12**, **14**, or **15** in quantitative yield as determined by NMR spectroscopy.

[(μ²-(1,4-(Ph₂PCH₂CH₂O)₂-2,3,5,6-((CH₃)₄C₆))₂(CO)₂(CH₃CN)₂Rh₂][BF₄]₂ (12). Slow diffusion of Et₂O into a CH₃CN solution of **12** yielded yellow blades that were characterized via X-ray crystallography. ¹H NMR: (CD₂Cl₂) δ 7.72 (m, 16H, P(C₆H₅)₂), 7.49 (m, 24H, P(C₆H₅)₂), 4.03 (m, 8H, CH₂P), 3.17 (m, 8H, CH₂O), 2.01 (s, 24H, CH₃) 1.62 (s, 6H, CH₃CN). ³¹P{¹H} NMR: (CD₂Cl₂) δ 20.5 (d, J_{Rh-P} = 117 Hz). FT-IR: (CD₂Cl₂) ν_{CO} = 2008 cm⁻¹ (s), 1971 cm⁻¹ (w). MS(ES): [[M²⁺][BF₄⁻] - CH₃CN]⁺ calcd = 1570.3, expt = 1571.0 m/z.

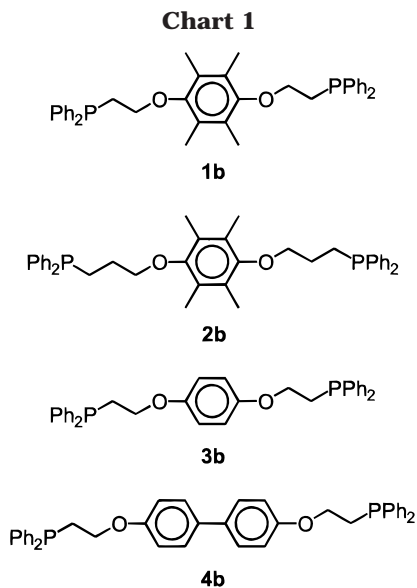
Synthesis of [(μ²-(1,4-(Ph₂PCH₂CH₂O)₂-2,3,5,6-((CH₃)₄-C₆))₂(CO)₂(CH₃CN)₂Rh₂][BF₄]₂ (13). To an NMR tube containing **6** (0.010 g, 0.00062 mmol) in CD₂Cl₂ (0.7 mL) was added one drop of CH₃CN followed by exposure to CO (1 atm) for 2 h. The solvent was removed in vacuo, and the product was redissolved in CD₂Cl₂, yielding a yellow solution of **13** in quantitative yield as determined by NMR spectroscopy. ¹H NMR: (CD₂Cl₂) δ 7.68 (b, 16H, P(C₆H₅)₂), 7.56 (b, 24H, P(C₆H₅)₂), 3.71 (b, 8H, CH₂P), 2.88 (m, 8H, CH₂O), 2.08 (s, 24H, CH₃), 1.44 (b, 8H, CH₂CH₂CH₂), 1.26 (s, 6H, CH₃CN). ³¹P{¹H} NMR: (CD₂Cl₂) δ 25.4 (d, J_{Rh-P} = 114 Hz). FTIR: (CD₂Cl₂) ν_{CO} = 2009 cm⁻¹ (s), 1971 cm⁻¹ (w). MS(ES): [[M²⁺][BF₄⁻] - 2CH₃CN]⁺ calcd = 1523.4, expt = 1523.4.

[(μ²-(1,4-(Ph₂PCH₂CH₂O)₂-C₆H₄)₂(CO)₂(CH₃CN)₂Rh₂][BF₄]₂ (14). ¹H NMR: (CD₂Cl₂) δ 7.61 (m, 16H, P(C₆H₅)₂), 7.42 (m, 24H, P(C₆H₅)₂), 6.56 (s, 8H, CH), 4.27 (m, 8H, CH₂O), 3.01 (m, 8H, CH₂P), 1.97 (s, 6H, CH₃CN). ³¹P{¹H} NMR: (CD₂Cl₂) δ 23.2 (J_{Rh-P} = 123 Hz). FT-IR: (CD₃CN) ν_{CO} = 2011 cm⁻¹ (s), 1979 cm⁻¹ (w). MS(ES): [[M²⁺][BF₄⁻] - CH₃CN]⁺ calcd = 1458.2, expt 1458.2 m/z.

[(μ²-(4,4'-(Ph₂PCH₂CH₂O)₂-C₆H₄-C₆H₄)₂(CO)₂(CH₃CN)₂Rh₂][BF₄]₂ (15). ¹H NMR: (CD₂Cl₂) δ 7.70 (b, 16H, P(C₆H₅)₂), 7.53 (b, 24H, P(C₆H₅)₂), 7.23 (d, 8H, C₆H₄, J_{H-H} = 8.7 Hz), 6.65 (d, 8H, C₆H₄, J_{H-H} = 8.8 Hz), 4.46 (b, 8H, CH₂O), 3.14 (b, 8H, CH₂P), 1.73 (s, 6H, CH₃CN). ³¹P{¹H} NMR: (CD₂Cl₂) δ 23.8 (d, J_{Rh-P} = 123 Hz). MS(ES): [[M²⁺][BF₄⁻]-2CH₃CN]⁺ calcd = 1569.2, expt = 1569.2, [M]²⁺ calcd = 782.1, expt = 782.1, [M²⁺-CH₃CN] calcd = 761.6, expt = 761.7 m/z.

Synthesis of [(μ²-(1,4-(Ph₂PCH₂CH₂O)₂-2,3,5,6-((CH₃)₄-C₆))₂(CO)₂(μ²-1,4-(NC)₂C₆H₄)Rh₂][BF₄]₂ (16). One equivalent (64 μL) of a 0.1 M solution of 1,4-dicyanobenzene (0.0128 g in 1.0 mL of CD₂Cl₂) was added to a solution of **9** (0.011 g, 0.0064 mmol) in CD₂Cl₂ (0.7 mL), leading to clean and quantitative formation of complex **16** as determined by ³¹P{¹H} and ¹H NMR spectroscopy. ¹H NMR: (CD₂Cl₂) δ 7.70 (m, 16H, P(C₆H₅)₂), 7.53 (m, 24H, P(C₆H₅)₂), 7.20 (b, 4H, 1,4-C₆H₄), 4.03 (m, 8H, CH₂O), 3.14 (m, 8H, CH₂P), 2.00 (s, 24H, CH₃).

Synthesis of [(μ²-(1,4-(Ph₂PCH₂CH₂O)₂-2,3,5,6-((CH₃)₄-C₆))₂(CH₃CN)₂(μ²-1,4-(NC)₂C₆H₄)Rh₂][BF₄]₂ (17). One equivalent of 1,4-phenylene diisocyanide (0.82 mg, 0.0064 mmol) was added to a solution of **5a** (0.010 g, 0.0064 mmol) in CD₂Cl₂ (0.7 mL) in an NMR tube, which immediately resulted in the formation of an orange precipitate. Addition of 10 equiv of CH₃CN (3.3 μL, 0.064 mmol) and vigorous shaking led to the slow (7 days) transformation to **17** in quantitative yield as determined by NMR spectroscopy. Single crystals of **17** were grown by diffusion of pentane into a saturated solution of



CD_2Cl_2 and were characterized by X-ray crystallography. ^1H NMR: (CD_2Cl_2) δ 7.70 (m, 16H, $\text{P}(\text{C}_6\text{H}_5)_2$), 7.53 (m, 24H, $\text{P}(\text{C}_6\text{H}_5)_2$), 5.96 (s, 4H, 1,4-(CN) $_2\text{C}_6\text{H}_4$), 3.54 (m, 8H, CH_2O), 3.27 (m, 8H, CH_2P), 1.80 (s, 24H, CH_3), 0.99 (s, 6H, CH_3CN). $^{31}\text{P}\{^1\text{H}\}$ NMR: (CD_2Cl_2) δ 18 (d, $J_{\text{Rh-P}} = 125$ Hz). MS(ES): $[\text{M}]^{2+}$ calcd = 798.2, expt = 798.3 m/z , $[\text{M}^{2+} - (\text{CH}_3\text{CN})]^{2+}$ calcd = 777.7, expt = 777.9 m/z , $[\text{M}^{2+} - 2(\text{CH}_3\text{CN})]^{2+}$ calcd = 757.2, expt = 757.3 m/z .

Results

Ligands 1b–4b. The four new ligands used in this study, **1b–4b** (Chart 1), were prepared using a simple two-step methodology (see Experimental Section) and have been fully characterized by ^1H and $^{31}\text{P}\{^1\text{H}\}$ NMR spectroscopy, mass spectrometry, and melting point analyses. All are moderately air-stable white solids that can be prepared readily on gram scales.

Synthesis and Characterization of Condensed Macrocycles 5a–c. There are many distinct structural motifs that can result from the reaction of ligand **1b** with a Rh(I) starting material, three of which have been characterized herein, **5a–c** in Scheme 2. However, reaction conditions can be used to significantly affect the product distribution. For example, the cis-phosphine cis-ether condensed binuclear macrocycle, **5a**, can be prepared selectively by combining a source of mononuclear Rh(I), $[\text{Rh}(\mu\text{-Cl})(\text{COE})_2]_2/\text{AgBF}_4$, with **1b** in THF at -78 °C. After the addition of **1b**, the solution is warmed to room temperature, and then the solvent is removed in vacuo. ^1H and $^{31}\text{P}\{^1\text{H}\}$ NMR spectroscopy show that under these conditions *only* **5a** is formed. Compound **5a** has been fully characterized in solution (see Experimental Section) and in the solid-state by a single-crystal X-ray diffraction study (vide infra).²⁴

Compound **5a** is only slightly soluble in THF. Refluxing a solution of **5a** in THF results in a slow conversion of **5a** into **5b** as a function of reaction time. Compound **5b** is characterized by two sets of doublets of doublets at δ 34.1 ($J_{\text{P-P}} = 40$ Hz, $J_{\text{Rh-P}} = 201$ Hz) and δ 20.3 ($J_{\text{P-P}} = 40$ Hz, $J_{\text{Rh-P}} = 210$ Hz) in its $^{31}\text{P}\{^1\text{H}\}$ NMR spectrum, which are assigned to the magnetically inequivalent P atoms. After 4 h, the reaction mixture consists of a 1:3 ratio of **5a** to **5b** and a small amount of decomposition (5–10%), as evidenced by the formation

of a brown precipitate. Note that because of its symmetry, compound **5a** shows only one resonance in its $^{31}\text{P}\{^1\text{H}\}$ NMR spectra (δ 61.4 (d, $J_{\text{Rh-P}} = 213$ Hz)) due to its magnetically equivalent P atoms. The chemical shift and coupling constants associated with the resonances in the $^{31}\text{P}\{^1\text{H}\}$ NMR spectrum of **5b** compare well with those observed in the spectra of analogous mononuclear cis-phosphine η^6 -arene Rh(I) compounds reported previously such as $[\text{Rh}(\eta^6:\eta^1\text{-PhO}(\text{CH}_2)_2\text{PPh}_2)(\eta^1\text{-PhO}(\text{CH}_2)_2\text{PPh}_2)]\text{BF}_4$ ($\delta = 32.6, 34.9$, $J_{\text{Rh-P}} = 198.7, 210.4$ Hz) and $[\text{Rh}(\eta^6:\eta^1\text{-Ph}(\text{CH}_2)_3\text{PPh}_2)(\eta^1\text{-Ph}(\text{CH}_2)_3\text{PPh}_2)]\text{BF}_4$ ($\delta = 36.6, 39.8$, $J_{\text{Rh-P}} = 203.9, 198.8$ Hz).³³

Although at room temperature **5a** and **5b** appear to be stable indefinitely, they do rearrange in $\text{ClCD}_2\text{CD}_2\text{-Cl}$ to form **5c** if heated at 75 °C for 10 days. The reactions are accompanied by a small degree (10–20%) of decomposition. Complex **5c** has been isolated and characterized by ^1H and $^{31}\text{P}\{^1\text{H}\}$ NMR spectroscopy, MS(ES), and a single-crystal X-ray diffraction study.

Solid-State Structures of 5a and 5c. The solid-state structure of **5a** has been determined via a single-crystal X-ray diffraction study²⁴ and is consistent with its solution structure (Figure 1). Despite several recrystallizations, the best crystals obtained were extremely weak diffractors, and the reflections were diffuse. The dication is located on a 2-fold axis. One anion is located on a 3-fold axis, with one of the fluorine atoms equally disordered over two positions. The second anion is disordered over a 2-fold axis and was refined isotropically. Both anions were refined as rigid tetrahedra with averaged boron–fluorine distances. The third anion is disordered over 2-fold and 3-fold axes with only one unique atom that was modeled as an oversized fluorine atom, labeled BF, and refined isotropically. Thus, a total anionic charge of -1 is assembled from $1/3$, $1/2$, and $1/6$ of a BF_4^- anion.

Compound **5a** is comprised of a series of five-membered rings, a ring size that is relatively free of strain in inorganic and organometallic systems.³⁴ The durenyl (1,2,4,5-tetramethylbenzene) rings of complex **5a** are parallel planar and separated by a distance of 3.32 Å, which is similar to the interlayer separation of graphite, 3.35 Å.³⁴ This distance between the two durene rings of **5a** is within the range typically associated with π - π stacking interactions.^{35,36} These two factors contribute to the stability of **5a**, a moderately air-sensitive but easily isolable compound.

Orange prismatic single crystals of **5c** suitable for X-ray diffraction studies were grown by diffusion of Et_2O into a saturated solution of **5c** in CH_2Cl_2 . An ORTEP diagram of **5c** along with selected bond distances and angles is shown in Figure 2, and important crystallographic parameters are presented in Table 1. The durene ring of **5c** is not planar (average deviation = 0.0476 Å) and has adopted a boat configuration with two short ($\text{Rh}(1)\text{-C}(3) = 2.240(2)$ Å, $\text{Rh}(1)\text{-C}(6) = 2.234(2)$ Å) and four long ($\text{Rh}(1)\text{-C}(4) = 2.357(2)$ Å, $\text{Rh}(1)\text{-C}(5) = 2.382(2)$ Å, $\text{Rh}(1)\text{-C}(7) = 2.333(2)$ Å,

(33) Singewald, E. T.; Mirkin, C. A.; Levy, A. D.; Stern, C. L. *Angew. Chem., Int. Ed. Engl.* **1994**, *33*, 2473–2475.

(34) Shriver, D. F.; Atkins, P.; Langford, C. H. *Inorganic Chemistry*, 2nd ed.; W. H. Freeman: New York, 1997.

(35) Claessens, C. G.; Stoddart, J. F. *J. Phys. Org. Chem.* **1997**, *10*, 254–272.

(36) Dahl, T. *Acta Chem. Scand.* **1994**, *48*, 95–106.

Scheme 2

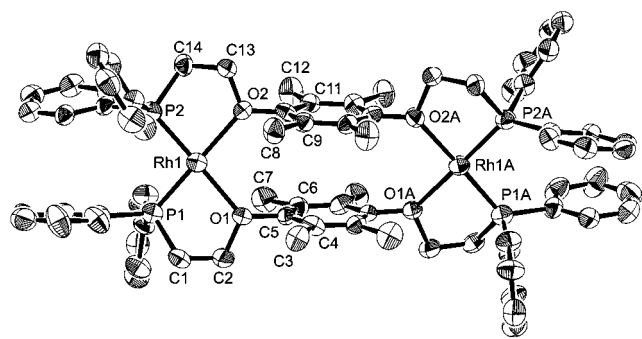
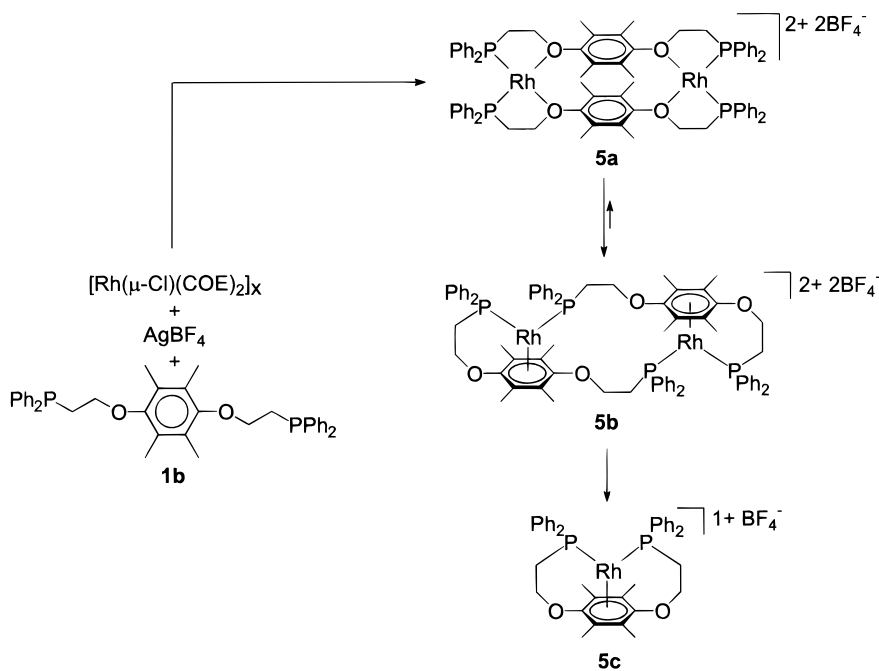


Figure 1. ORTEP diagram of **5a** showing atom-labeling scheme. Unlabeled atoms follow same numbering scheme as labeled atoms. Thermal ellipsoids are shown at 30% probability. Counterions and hydrogen atoms are omitted for clarity. Selected bond distances (Å) and angles (deg): Rh(1)–Rh(1a) = 8.362(10); Rh(1)–P(1) = 2.169(3); Rh(1)–P(2) = 2.172(3); Rh(1)–O(1) = 2.247(7); Rh(1)–O(2) = 2.217(7); P(1)–Rh(1)–P(2) = 98.35(12); P(1)–Rh(1)–O(1) = 81.3(2); P(1)–Rh(1)–O(2) = 174.8(2); P(2)–Rh(1)–O(1) = 173.9(2); P(2)–Rh(1)–O(2) = 82.3(2); O(1)–Rh(1)–O(2) = 98.7(2).

Rh(1)–C(8) = 2.362(2) Å Rh–C bonds (average Rh–C bond length = 2.318 Å). This deviation from planarity is almost twice as large as the deviations of analogous structures reported previously by our group (four structures, average deviation from planarity = 0.0169–0.0240 Å).^{37,38} The bow and the stern of the “boat” correspond to the two C atoms that are bound to O atoms and point toward the rhodium atom. The average Rh–P bond distance (2.2388(12) Å) of **5c** falls within the range of previously reported mononuclear Rh(I) η^6 -arene two-legged piano-stool structures (average Rh–P bond distances = 2.219–2.251 Å).^{32,37–42}

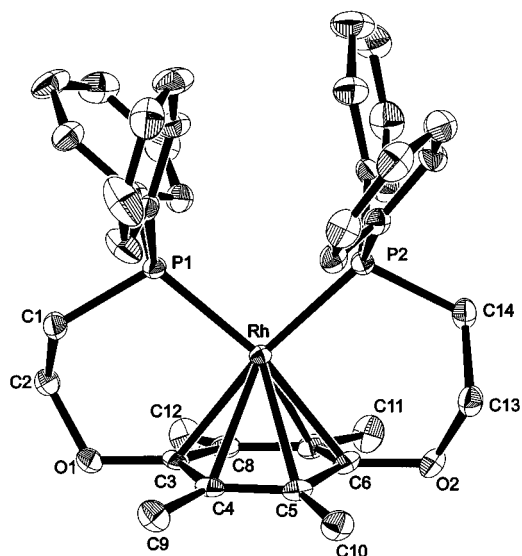


Figure 2. ORTEP diagram of **5c** showing atom-labeling scheme. Unlabeled atoms follow same numbering scheme as labeled atoms. Thermal ellipsoids are shown at 30% probability. Counterions and hydrogen atoms are omitted for clarity. Selected bond distances (Å) and angles (deg): Rh(1)–P(1) = 2.2327(6); Rh(1)–P(2) = 2.2449(6); Rh(1)–arene = 1.83(2); Rh(1)–C(3) = 2.240(2); Rh(1)–C(4) = 2.357(2); Rh(1)–C(5) = 2.382(2); Rh(1)–C(6) = 2.234(2); Rh(1)–C(7) = 2.333(2); Rh(1)–C(8) = 2.362(2); P(1)–Rh(1)–P(2) = 96.48(2).

Synthesis and Characterization of 6, 7, and 8. Combination of ligands **2b–4b** with $[\text{Rh}(\mu\text{-Cl})(\text{COE})_2]_x/\text{AgBF}_4$ under similar conditions used to form **5a** results in the formation of **6–8**, respectively (Chart 2). Com-

(39) Slone, C. S.; Mirkin, C. A.; Yap, G. P. A.; Guzei, I. A.; Rheingold, A. L. *J. Am. Chem. Soc.* **1997**, *119*, 10743–10753.

(40) Sassano, C. A.; Mirkin, C. A. *J. Am. Chem. Soc.* **1995**, *117*, 11379–11380.

(41) Singewald, E. T.; Mirkin, C. A.; Stern, C. L. *Angew. Chem., Int. Ed. Engl.* **1995**, *34*, 1624–1627.

(42) Allgeier, A. M.; Singewald, E. T.; Mirkin, C. A.; Stern, C. L. *Organometallics* **1994**, *13*, 2928–2930.

(37) Singewald, E. T.; Slone, C. S.; Stern, C. L.; Mirkin, C. A.; Yap, G. P. A.; Liable-Sands, L. M.; Rheingold, A. L. *J. Am. Chem. Soc.* **1997**, *119*, 3048–3056.

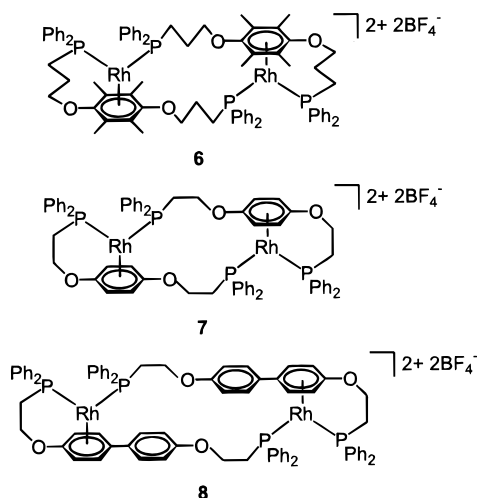
(38) Singewald, E. T.; Shi, X.; Mirkin, C. A.; Schofer, S. J.; Stern, C. L. *Organometallics* **1996**, *15*, 3062–3069.

Table 1. Crystallographic Data

	5a	5c	6·2.5CH ₂ Cl ₂	9	10·6CH ₂ Cl ₂	12·2Et ₂ O	17·CH ₂ Cl ₂ ·3Et ₂ O
formula	C ₇₆ H ₈₀ B ₂ F ₈ O ₄ ·P ₄ Rh ₂	C ₃₈ H ₄₀ BF ₄ O ₂ ·P ₂ Rh	C _{82.5} H ₉₃ B ₂ Cl ₅ F ₈ ·O ₄ P ₄ Rh ₂	C ₈₂ H ₈₀ B ₂ F ₈ O ₁₀ ·P ₄ Rh ₂	C ₈₀ H ₇₆ B ₂ Cl ₁₂ F ₈ ·O ₁₀ P ₄ Rh ₂	C ₉₀ H ₁₀₆ B ₂ F ₈ N ₂ O ₈ ·P ₄ Rh ₂	C ₁₀₁ H ₁₂₂ B ₂ Cl ₂ F ₈ ·N ₄ O ₇ P ₄ Rh ₂
fw	1560.72	780.39	1829.14	1728.78	2126.13	1847.09	2078.23
crystal system	trigonal	triclinic	monoclinic	monoclinic	triclinic	triclinic	tetragonal
space group	<i>P</i> 31 <i>c</i>	<i>P</i> 1̄	<i>C</i> 2/ <i>c</i>	<i>C</i> 2/ <i>c</i>	<i>P</i> 1̄	<i>P</i> 1̄	<i>P</i> 4 ₁ 2 ₁ 2
color	orange	orange	red	yellow	pale yellow	pale yellow	yellow
temp, K	218(2)	153(1)	173(2)	173(2)	203(2)	223(2)	223(2)
<i>a</i> , Å	22.9145(5)	10.534(3)	31.1605(5)	43.1098(8)	11.4372(2)	10.5002(2)	16.6807(1)
<i>b</i> , Å		11.731(3)	21.2133(2)	11.1044(2)	12.5022(3)	12.0452(2)	
<i>c</i> , Å	26.4671(9)	14.669(3)	32.5273(2)	20.7096(3)	17.1864(3)	18.6589(1)	39.1582(1)
α , deg		87.21(2)			93.7130(2)	95.392(1)	
β , deg		86.64(2)	105.1385(8)	118.523(1)	96.4527(7)	95.591(1)	
γ , deg		72.84(2)			108.8376(7)	104.171(1)	
<i>V</i> , Å ³	12035.3(6)	1728.1(8)	20754.9(4)	8710.6(3)	2297.76(11)	2260.18(6)	10895.60(10)
<i>Z</i>	6	2	8	4	1	1	4
<i>R</i> ^a , <i>R</i> _w ^b	0.0999, 0.2098	0.022, 0.027 ^A	0.0681, 0.1964	0.0734, 0.1580	0.0626, 0.1697	0.0376, 0.1185	0.0733, 0.1825
GOF	0.952	2.92	1.514	0.917	1.506	1.158	1.180

^A *R*_w^b is instead *R*_w^a.

Chart 2



pounds **6–8** are condensed binuclear macrocycles with η^6 -arene two-legged piano-stool geometries about their metal centers. Complexes **6–8** have been characterized via ¹H and ³¹P{¹H} NMR spectroscopy, MS(ES), and, in the case of **6** and **7**, single-crystal X-ray diffraction studies, and all data are consistent with our proposed structural formulations.

The ³¹P{¹H} NMR spectra of **6–8** show a pair of doublet of doublets at δ 28.3 (dd, $J_{P-P} = 42$ Hz, $J_{Rh-P} = 203$ Hz) and δ 23.8 (dd, $J_{P-P} = 42$ Hz, $J_{Rh-P} = 209$ Hz) for **6**, δ 34.8 (dd, $J_{P-P} = 38$ Hz, $J_{Rh-P} = 206$ Hz) and δ 27.3 (dd, $J_{P-P} = 38$ Hz, $J_{Rh-P} = 213$ Hz) for **7** and δ 33.0 (dd, $J_{P-P} = 39$ Hz, $J_{Rh-P} = 203$ Hz) and δ 25.9 (dd, $J_{P-P} = 39$ Hz, $J_{Rh-P} = 213$ Hz) for **8**. In general, the resonances in the ³¹P{¹H} NMR spectra of the two compounds derived from durene ligands (**5b** and **6**) exhibit chemical shifts that are slightly upfield, have slightly larger P–P coupling constants, and have slightly smaller Rh–P coupling constants than the two structures, **7** and **8**, derived from C₆H₄-type ligands. The ³¹P{¹H} NMR spectra of model mononuclear Rh(I) compounds with piano-stool geometry and that of **5b** compare well with the spectra of **7** and **8**.^{33,37–42} Most notably, they all exhibit similar chemical shifts and coupling constants consistent with their nearly identical ligand environments about the Rh(I) metal centers.

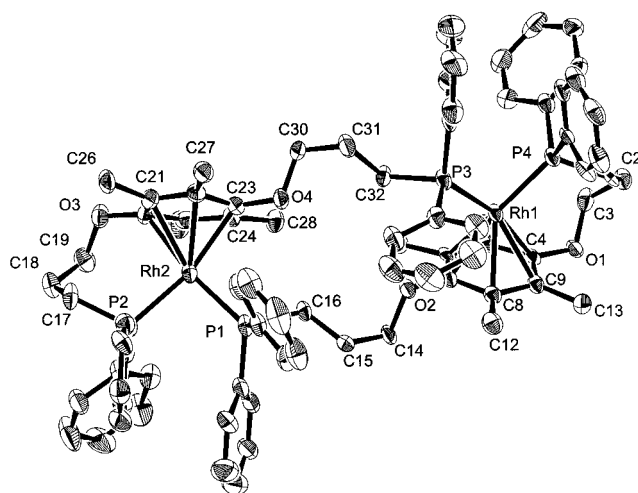


Figure 3. ORTEP diagram of **6**·2.5CH₂Cl₂ showing atom-labeling scheme. Unlabeled atoms follow same numbering scheme as labeled atoms. Thermal ellipsoids are shown at 30% probability. Counterions, solvent molecules, and hydrogen atoms are omitted for clarity. Selected bond distances (Å) and angles (deg): Rh(1)–P(4) = 2.2513(16); Rh(1)–P(4) = 2.2539(15); Rh(1)–C(4) = 2.301(6); Rh(1)–C(4) = 2.437(5); Rh(1)–C(6) = 2.402(5); Rh(1)–C(7) = 2.269(6); Rh(1)–C(8) = 2.329(6); Rh(1)–C(9) = 2.352(6); Rh(2)–P(1) = 2.2707(17); Rh(2)–P(2) = 2.2537(18); Rh(2)–C(20) = 2.311(6); Rh(2)–C(21) = 2.375(6); Rh(2)–C(22) = 2.417(6); Rh(2)–C(23) = 2.298(6); Rh(2)–C(24) = 2.370(6); Rh(2)–C(25) = 2.435(7); P(1)–Rh(2)–P(2) = 92.77(6); P(3)–Rh(1)–P(4) = 95.88(6).

Solid-State Structure of 6. The solid-state structure of **6**·2.5CH₂Cl₂ has been determined via a single-crystal X-ray diffraction study (Figure 3). As in **5c**, the η^6 -arenes of **6** experience a boatlike distortion, with two short bonds and four long bonds. The two shorter Rh–C bonds involve atoms C(10) and C(11), which are attached to the O atoms (Figure 3). The mean deviations of the η^6 -arenes from planarity are smaller for **6** (0.0305 Å for the ring defined by C4–C9 and 0.0357 Å for the ring defined by C20–C21) than for **5c** (0.0476 Å). The arene rings of **6** also are slightly farther away from the Rh(I) metal centers with an average distance of 1.89 Å for **6** compared to a separation of 1.83 Å for **5c**. The shorter Rh(I)–arene distance for **5c** is attributed to the chelation of the durenyl moiety to both phosphines of

Scheme 3

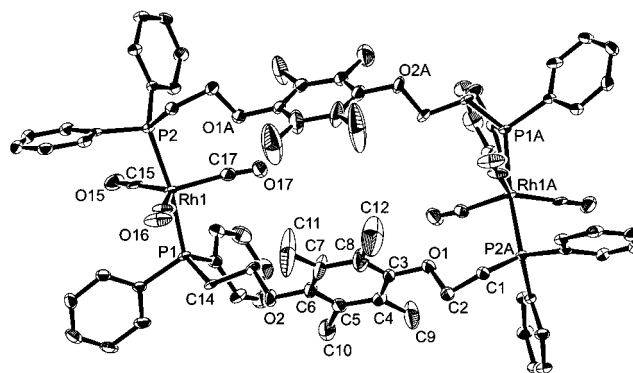
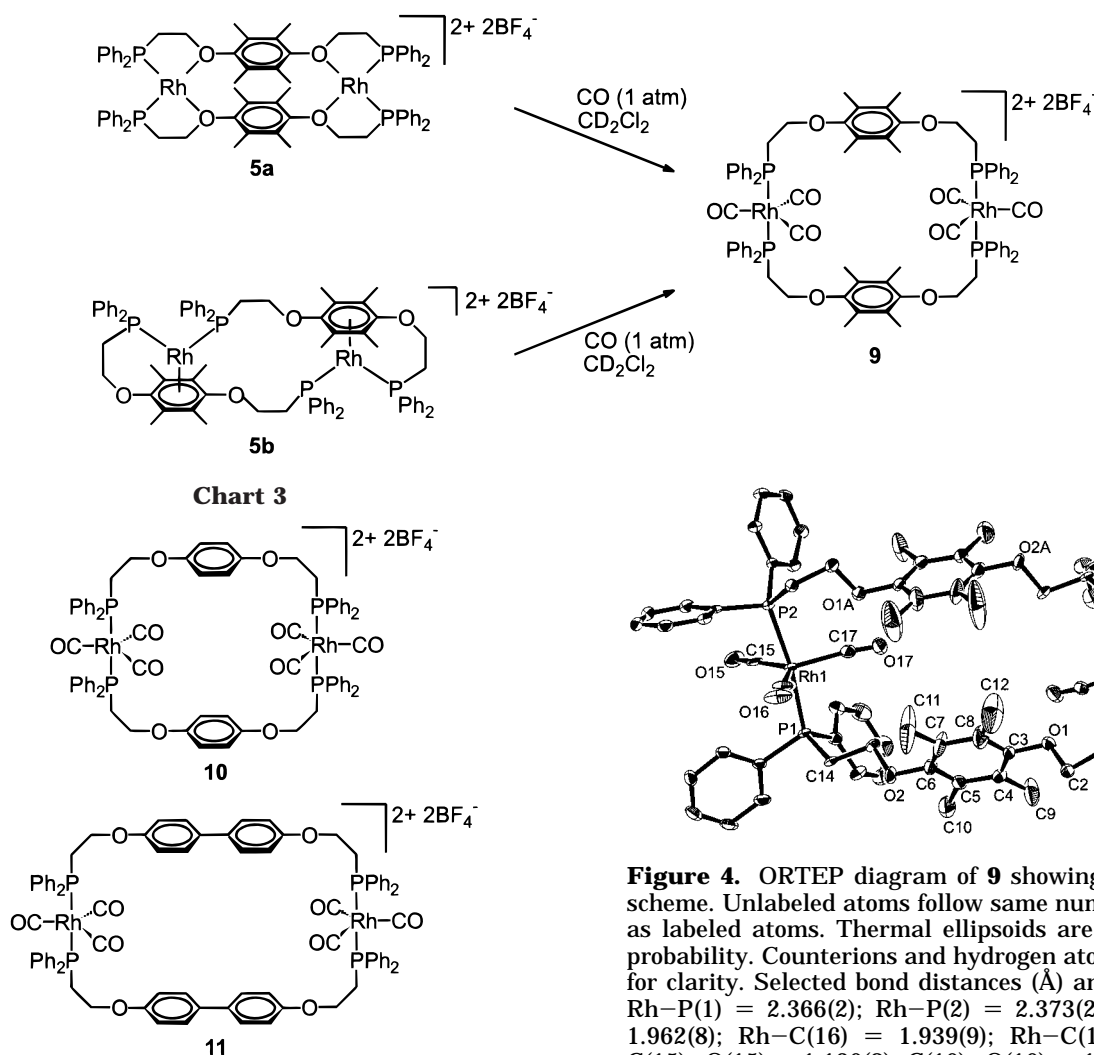


Figure 4. ORTEP diagram of **9** showing atom-labeling scheme as labeled atoms. Unlabeled atoms follow same numbering scheme as labeled atoms. Thermal ellipsoids are shown at 30% probability. Counterions and hydrogen atoms are omitted for clarity. Selected bond distances (Å) and angles (deg): Rh–P(1) = 2.366(2); Rh–P(2) = 2.373(2); Rh–C(15) = 1.962(8); Rh–C(16) = 1.939(9); Rh–C(17) = 2.045(8); C(15)–O(15) = 1.126(8); C(16)–O(16) = 1.111(9); C(17)–O(17) = 1.109(8); P(1)–Rh–P(2) = 171.92(6); C(15)–Rh–C(16) = 132.3(3); C(16)–Rh–C(17) = 114.7(3); C(17)–Rh–C(15) = 113.0(3); C(15)–Rh–P(1) = 89.4(2); C(16)–Rh–P(1) = 89.0(2); C(17)–Rh–P(1) = 90.3(2); C(15)–Rh–P(2) = 88.6(2); C(16)–Rh–P(2) = 86.5(2); C(17)–Rh–P(2) = 97.7(2).

the mononuclear complex, which effectively pulls the arene closer to the Rh(I) metal center.

Synthesis and Characterization of Hexa-CO Adducts 9–11. Exposure of CH₂Cl₂ solutions of complexes **5a**, **5b**, **7**, and **8** to CO (1 atm) leads to breaking of the relatively weak rhodium–η¹-ether or rhodium–η⁶-arene bonds and quantitative formation of the open 26- and 34-membered macrocyclic ring structures **9–11** (Scheme 3 and Chart 3). Note that both **5a** and **5b** are precursors for the metallomacrocyclic complex **9** (Scheme 3). The binuclear macrocycles each contain trigonal bipyramidal metal centers where two phosphine ligands occupy the axial sites and three CO moieties occupy the equatorial sites. In all cases, **9–11** were formed in two steps (formation of a condensed macrocycle followed by ring-opening with CO), allowing for the complete characterization of intermediates **5a**, **5b**, **7**, and **8**, but it is important to note that **9–11** also have been formed in one-pot reactions without the isolation of these condensed macrocycle intermediates. Compounds **9–11** have been characterized by ¹H and ³¹P{¹H} NMR spectroscopy, and although the lability of the CO ligands in these complexes preclude their characterization via mass spectrometry methods, the solid-state structures of both **9** and **10** have been confirmed by single-crystal X-ray diffraction studies (vide infra).

Solid-State Structures of 9 and 10. An ORTEP diagram of **9** along with important bond lengths and angles is presented in Figure 4, while crystallographic data are in Table 1. The dication **9** is located on a crystallographic 2-fold axis. Three CO ligands are attached to each rhodium metal center in **9**, and the metal centers are separated by 11.64 Å. The two durenyl moieties are separated by 6.29 Å and are canted with respect to one another at an angle of 64°.

A single-crystal of **10**·6CH₂Cl₂ was grown from a CH₂Cl₂ solution of **10** under CO (1 atm). An ORTEP diagram of **10**·6CH₂Cl₂ and important bond lengths and angles are given in Figure 5, and crystallographic data are presented in Table 1. Complex **10** lies on a crystallographic inversion center. The average Rh–CO and Rh–P distances are both longer for complex **9** than those in **10** (average Rh–CO distance = 1.982(8) Å vs 1.959(5) Å, and average Rh–P distance = 2.370(2) Å vs 2.355(1) Å). The two Rh(I) metal centers in **10** are separated by a distance of 11.05 Å, and unlike the phenyl rings in **9**, which are canted with respect to one

Scheme 4

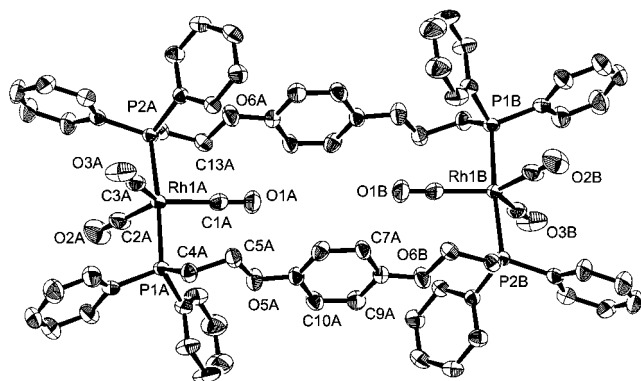
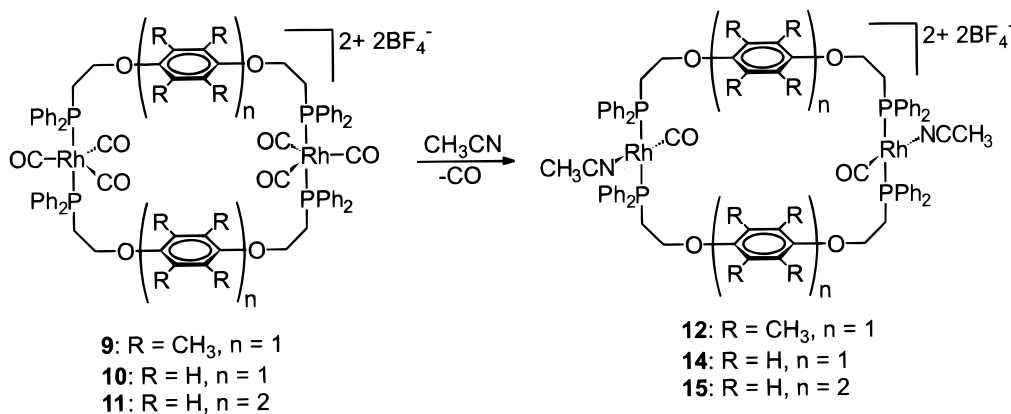
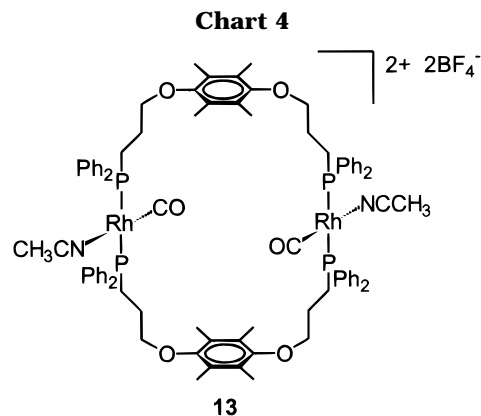


Figure 5. ORTEP diagram of **10**·6CH₂Cl₂ showing atom-labeling scheme. Unlabeled atoms follow same numbering scheme as labeled atoms. Thermal ellipsoids are shown at 30% probability. Counterions, solvent molecules, and hydrogen atoms are omitted for clarity. Selected bond distances (Å) and angles (deg): Rh(1)–P(1) = 2.3537(10); Rh(1)–P(2) = 2.3558(10); Rh–C(1) = 1.990(5); Rh–C(2) = 1.955(5); Rh–C(3) = 1.93(5); C(1)–O(1) = 1.108(6); C(2)–O(2) = 1.129(6); C(3)–O(3) = 1.133(6); P(1)–Rh–P(2) = 175.96(4); C(1)–Rh–C(2) = 119.3(2); C(2)–Rh–C(3) = 118.0(2); C(3)–Rh–C(1) = 122.7(2); C(1)–Rh–P(1) = 91.42(13); C(2)–Rh–P(1) = 89.48(14); C(3)–Rh–P(1) = 89.48(13); C(1)–Rh–P(2) = 92.62(13); C(2)–Rh–P(2) = 88.43(14); C(3)–Rh–P(2) = 88.44(13).

another, the two phenyl moieties of **10** are parallel-planar and separated by a distance of 6.58 Å.

Synthesis and Characterization of CH₃CN/CO Adducts 12–15. The steric and electronic environments around the Rh(I) metal centers of these macrocycles are easily controlled through ligand substitution reactions. For example, in compounds **9–11** two of the CO ligands at each Rh(I) metal center can be replaced by a nitrile ligand such as CH₃CN to form square-planar complexes **12**, **14**, and **15**, respectively (Scheme 4). Compound **13** was synthesized via a different method to demonstrate the multiple synthetic approaches available for preparing structurally similar macrocycles. In a one-pot reaction, **6** was first exposed to CH₃CN, followed by exposure to CO (1 atm), resulting in the 30-membered-ring compound **13** (Chart 4). For compounds **12–15**, each rhodium metal center is bound to two trans-phosphines and trans CO and CH₃CN ligands. This ligand geometry is favorable due to the “push–pull” effect of the trans σ -donating (CH₃CN) and π -accepting (CO) ligands and has been observed and exploited extensively in organo-



metallic chemistry.^{43,44} Compounds **12–15** have been characterized by ¹H and ³¹P{¹H} NMR spectroscopy, MS(ES), and, in the case of **12**, a single-crystal X-ray diffraction study.

Solid-State Structure of 12. Important bond lengths and angles along with an ORTEP diagram of **12**·2Et₂O are presented in Figure 6, and the crystallographic data are presented in Table 1. As in the structure for **5a**, the durenyl rings are nearly parallel-planar but are now separated by a distance of 6.44 Å, and the two rhodium metal centers are separated by 11.61 Å. The solid-state structure of **12**·2Et₂O is the proposed solution structure and clearly shows that the Rh(I) metal centers are square planar with trans-phosphines and the CH₃CN and CO ligands are in an anti conformation. The ³¹P{¹H} NMR spectrum of **12** exhibits a single doublet, which is unchanged down to temperatures of –50 °C, indicating a single conformation or an exceptionally facile interconversion of multiple conformational isomers. Comparison of the FT-IR spectrum of **12** (ν = 2008 cm⁻¹ (s), 1971 cm⁻¹ (w)) with other binuclear Rh(I) ring structures with syn and anti conformations indicates that the anti conformation observed in the solid state is maintained in solution.⁴⁵

Synthesis and Characterization of 16 and 17. The synthesis of macrocyclic complexes with coordinatively labile ligands provides the opportunity to use such structures to bind bifunctional aromatic molecules within their cavities by coordination chemistry. Addition

(43) Kim, M.; Chin, J.; Ko, J. *Bull. Korean Chem. Soc.* **1992**, *13*, 556–559.

(44) Schrock, R. R.; Osborn, J. A. *J. Am. Chem. Soc.* **1971**, *93*, 2397–2407.

(45) Sanger, A. R. *J. Chem. Soc., Dalton Trans.* **1976**, 120–129.

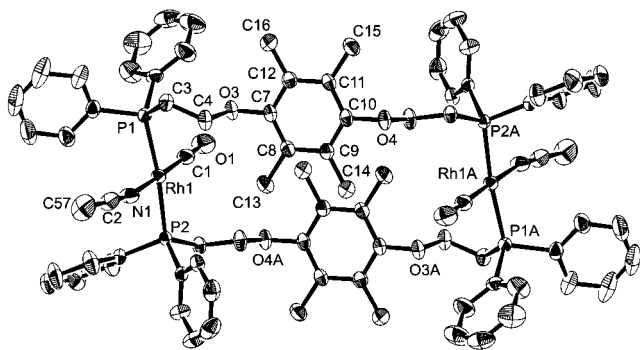


Figure 6. ORTEP diagram of **12**·2Et₂O showing atom-labeling scheme. Unlabeled atoms follow same numbering scheme as labeled atoms. Thermal ellipsoids are shown at 30% probability. Counterions, solvent molecules, and hydrogen atoms are omitted for clarity. Selected bond distances (Å) and angles (deg): Rh(1)–P(1) = 2.3238(6); Rh(1)–P(2) = 2.3291(6); Rh(1)–C(1) = 1.821(3); C(1)–O(1) = 1.147(3); Rh(1)–N(1) = 2.076(2); N(1)–C(2) = 1.136(4); C(2)–C(57) = 1.465(4); P(1)–Rh(1)–P(2) = 173.50(2); C(1)–Rh(1)–N(1) = 175.57(10); C(1)–Rh(1)–P(1) = 89.73(8); C(1)–Rh(1)–P(2) = 91.61(8); N(1)–Rh(1)–P(1) = 86.97(6); N(1)–Rh(1)–P(2) = 92.00(6); Rh(1)–C(1)–O(1) = 178.2(3); Rh(1)–N(1)–C(2) = 168.8(2); N(1)–C(2)–C(57) = 178.3(3).

of 1 equiv of 1,4-dicyanobenzene to **9** leads to quantitative formation of complex **16**, where the bifunctional aromatic dicyanide bridges the Rh(I) centers of a single macrocycle (Scheme 5). Again, this complex makes use of the push–pull effect (vide supra) by aligning σ -donating (1,4-dicyanobenzene) and π -accepting (CO) ligands trans to one another about the metal center. Confirmation of the structure of **16** was determined by ¹H NMR data, which shows diagnostic upfield shifts of δ 0.6 in the resonances assigned to the H atoms of 1,4-dicyanobenzene as compared with the free ligand. This is indicative of shielding interactions between the 1,4-dicyanobenzene and the durenyl moieties of **16**.⁴⁶ Further spectroscopic evidence for this structure was difficult to obtain due to the lability of the sequestered aromatic dinitrile. The ³¹P{¹H} NMR of **16** shows a doublet at δ 19.0 ($J_{\text{Rh-P}} = 115$ Hz), which compares well with **12** (δ 21.5 (d, $J_{\text{Rh-P}} = 117$ Hz)), a somewhat analogous structure in that both macrocycles are square planar with trans-phosphines, a CO ligand, and a σ -donating nitrile ligand. Cyano groups in general bind rather weakly to Rh(I) metal centers and are often broken under mass spectrometry conditions.²³

A much more robust complex was synthesized using 1,4-phenylenediisocyanide instead of 1,4-dicyanobenzene. The isocyanide group is known to bind to Rh(I) much more strongly than the cyano group.^{23,47} In a typical experiment, 1 equiv of 1,4-phenylenediisocyanide was added to a CD₂Cl₂ solution of **5a**, which resulted in the immediate formation of an orange precipitate (Scheme 5). Addition of excess CH₃CN (10 equiv) to the solution containing the orange precipitate led to quantitative formation of **17**, a macrocycle where the two rhodium metal centers of a single ring are spanned by

one bridging 1,4-phenylenediisocyanide molecule. This reaction demonstrates the ability of the metals in these novel binuclear macrocycles (or condensed intermediates) to guide the sequestration of bifunctional aromatic molecules that fit within the cage.

Complex **17** has been characterized by MS(ES), ¹H NMR, NOE difference, and ³¹P{¹H} NMR spectroscopy, along with a single-crystal X-ray diffraction study.²⁴ The ¹H NMR resonances on the 1,4-phenylenediisocyanide bound inside the macrocycle cavity are shifted upfield approximately δ 1.4 from the free ligand, which is indicative of π – π interactions between the aromatic groups of the macrocycle and the 1,4-phenylenediisocyanide.⁴⁶ Furthermore, the NOE ¹H difference spectrum shows through-space coupling between the methyl groups of the durenyl moieties of the macrocycle and the protons of the bound 1,4-phenylenediisocyanide (see Supporting Information).

Solid-State Structure of 17. Crystals of **17**·CH₂Cl₂·3Et₂O suitable for X-ray diffraction studies were grown by slow diffusion of pentane into a solution of **17** in CH₂Cl₂.²⁴ An ORTEP diagram of **17**·CH₂Cl₂·Et₂O, with important bond lengths and angles, is shown in Figure 7, and crystallographic data are presented in Table 1. The asymmetric unit consists of half a molecule of the dication, one BF₄ counterion, half a molecule of CH₂Cl₂, and a molecule and a half of Et₂O. The dication resides on a 2-fold axis. One solvate Et₂O molecule and the solvate CH₂Cl₂ molecule reside on 2-fold axes. The three aromatic groups of macrocycle **17** are parallel planar and separated by a distance of 4.24 Å.

Discussion

The weak-link approach to synthesizing inorganic macrocycles offers a new way of preparing metallomacrocyclic structures from transition metals and flexible hemilabile ligands (Scheme 1). Through the reactions studied and structures reported herein, we have identified several structural features that make a ligand particularly well suited for this synthetic methodology. First, the ligand should possess a group that will bind strongly to a metal center serving as an anchor holding the macrocycle together. For the first generation of ligands we have used phosphines and their predictable chemistry with late transition metals. Phosphines are known to bind strongly to Rh(I) metal centers, and their substituents offer a high degree of tailorability by allowing one to control both electronic and steric environments of the metal centers to which they are bound.⁴⁸ Second, one needs to strategically place a moiety within the ligand that will weakly bind to a metal center. It is important to consider favorable binding geometries when placing the weak link within a ligand since this weak link is responsible for allowing one to target a condensed macrocycle that can be formed in high yield (Scheme 1). Multidentate ligands that contain both strongly and weakly binding moieties are well-known in the literature and are often referred to as hemilabile ligands.^{37–42,49–53} In the cases reported here, we have found that both Rh– η^1 -ether and Rh– η^6 -arene interactions can serve as weak links.

We have chosen ligands **1b–4b** (Chart 1) to probe several factors regarding how ligand structure affects

(46) Anelli, P. L.; Ashton, P. R.; Ballardini, R.; Balzani, V.; Delgado, M.; Gandolfi, M. T.; Goodnow, T. T.; Kaifer, A. E.; Philp, D.; Pietraszkiewicz, M.; Prodi, L.; Reddington, M. V.; Slawin, A. M. Z.; Spencer, N.; Stoddart, J. F.; Vincent, C.; Williams, D. J. *J. Am. Chem. Soc.* **1992**, *114*, 193–218.

(47) Cotton, F. A.; Wilkinson, G. *Advanced Inorganic Chemistry*, 5th ed.; John Wiley & Sons: New York, 1988.

(48) Tolman, C. A. *Chem. Rev.* **1977**, *77*, 313–348.

Scheme 5

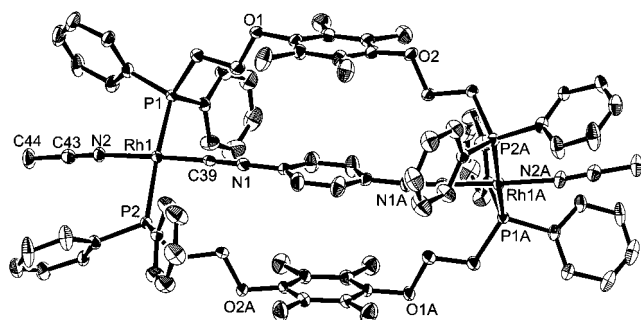
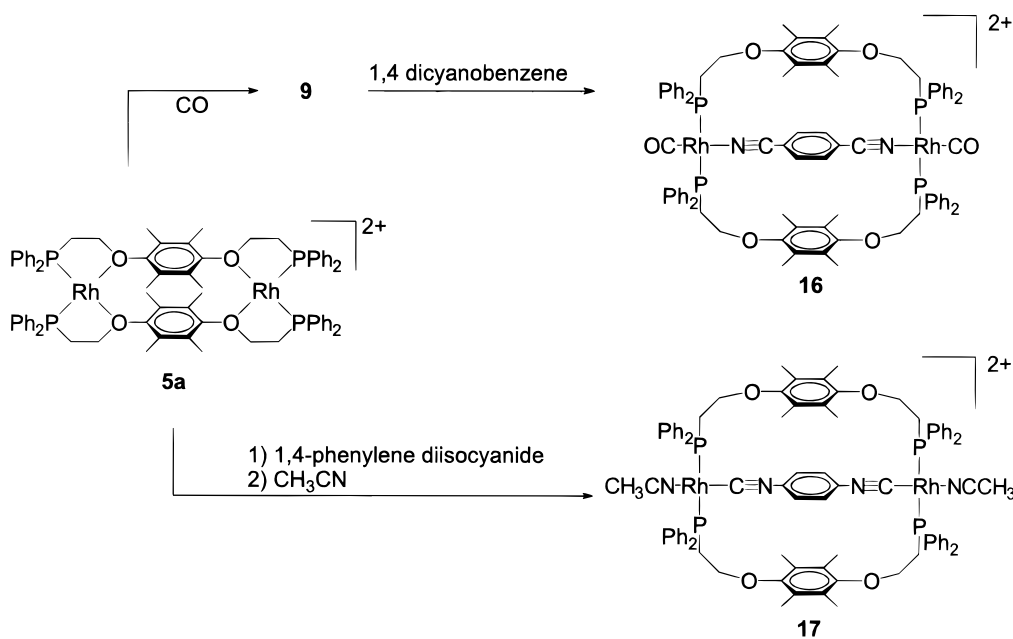


Figure 7. ORTEP drawing for complex $17 \cdot \text{CH}_2\text{Cl}_2 \cdot \text{Et}_2\text{O}$, with thermal ellipsoids drawn at the 30% probability level. Counterions, solvent molecules and hydrogen atoms are omitted for clarity. Selected bond distances (Å) and angles (deg): Rh(1)–Rh(1a) = 11.598(13); Rh(1)–P(1) = 2.343(6); Rh(1)–P(2) = 2.326(6); Rh(1)–N(2) = 2.06(2); Rh(1)–C(39) = 1.85(2); P(1)–Rh(1)–P(2) = 170.1(2); C(39)–Rh(1)–N(2) = 177.4(10); N(2)–Rh(1)–P(2) = 90.1(6); N(2)–Rh(1)–P(1) = 89.8(6); C(39)–Rh(1)–P(2) = 88.8(7); C(39)–Rh(1)–P(1) = 91.0(7).

the formation of the resulting macrocycles. This small set of ligands provides important insight into how size (phenyl vs biphenyl), electron richness of an arene (phenyl vs tetramethylphenyl), and steric factors can lead to macrocycles with different structural properties such as size, stability, and hydrophobicity of the macrocycle pocket.

The ligands for this study have been synthesized from both quinone and hydroquinone precursors. Quinones and hydroquinones are diverse, plentiful, and relatively inexpensive precursors that are often commercially

available, providing a means of easily and systematically varying ligand properties such as size, hydrophobicity, redox potentials, and other photophysical properties (e.g., optical activity). Ligands **1b–4b** demonstrate that both ethers and arenes function well as a weak link for Rh(I) metal centers. Additionally, they also show that functional groups within a ligand can have weak binding interactions toward each other that facilitate the formation of a particular type of condensed macrocycle. The condensed macrocycle **5a** has aromatic groups in close proximity, which allows π – π stacking interactions to further stabilize the structure. Including strategically placed aromatic groups in ligand design is advantageous for structures such as **5a**, where such groups can be used as a second weak-link to hold the condensed macrocycle together.

Although one must exercise careful control over the selection of reaction conditions, once conditions have been optimized, all of the macrocyclic structures can be synthesized in near quantitative yields (90–100%). In this weak-link approach, one is usually trying to synthesize a kinetic structure from a myriad of possible undesired structures. We have demonstrated how differences in solvents and reaction times result in the formation of some of these structures, especially in the case of **5a–5c** (Scheme 2). Specifically, combination of ligand **1b** with a mononuclear Rh(I) starting material in THF at -78°C over 1 h, followed by warming the reaction mixture to room temperature over 1 h, exclusively leads to compound **5a**. If instead of stopping the reaction at this point, one refluxes the reaction mixture, one observes a slow increase in the concentration of **5b** at the expense of **5a**. This interconversion between **5a** and **5b** does not require the breaking of any of the relatively strong Rh–P bonds; instead, it involves the intramolecular competition between the ether and aryl moieties of ligand **1b** for Rh(I) binding sites (Scheme 2).

Formation of **5c** is most efficiently effected by heating either a solution of **5a** or a solution of **5a** and **5b** in $\text{ClC}_2\text{D}_2\text{Cl}$ at 75°C for 10 days. At this elevated

(49) Slone, C. S.; Weinberger, D. A.; Mirkin, C. A. In *Progress in Inorganic Chemistry*; Karlin, K. D., Ed.; John Wiley & Sons: New York, 1999; Vol. 48, pp 233–350.

(50) Lindner, E.; Pautz, S.; Hausteiner, M. *Coord. Chem. Rev.* **1996**, *155*, 145–162.

(51) Bader, A.; Lindner, E. *Coord. Chem. Rev.* **1991**, *108*, 27–110.

(52) Allgeier, A. M.; Slone, C. S.; Mirkin, C. A.; Liabe-Sands, L. M.; Yap, G. P. A.; Rheingold, A. L. *J. Am. Chem. Soc.* **1997**, *119*, 550–559.

(53) Higgins, T. B.; Mirkin, C. A. *Inorg. Chim. Acta* **1995**, *240*, 347–353.

temperature, there is enough thermal energy to convert **5a** to **5b** (Scheme 2). The rearrangement of **5b** to form 2 equiv of **5c** could occur by breaking a single Rh–P bond at each Rh(I) metal center to form mononuclear products, followed by coordination of the now pendant P atom to the Rh(I) metal center. This rearrangement is less favorable in THF because compound **5a** has a very low solubility in THF, so once ligand **1b** and a Rh(I) starting material form **5a**, it precipitates from solution and the reaction is halted. All of these data lead one to conclude that **5a** and **5b** are kinetic products that are isolable due to a high barrier to forming the thermodynamic product, complex **5c** (Scheme 2).

Compounds **6–8** are all isolated cleanly as η^6 -piano-stool type complexes (Chart 2) from ligands **2b–4b** and a Rh(I) starting material. Compounds **6** and **7** are kinetic products, as evidenced by the fact that they rearrange to form mononuclear compounds similar to **5c** after extended periods of heating in $\text{ClCD}_2\text{CD}_2\text{Cl}$. These mononuclear complexes and their chemistry will be the subject of a future report. Regardless, under the conditions reported herein **6** and **7** can be prepared in quantitative yields and used as precursors to macrocycles **13** and **10**, respectively. Compound **8** does not rearrange to form a mononuclear compound, presumably because its chelating arms are not long enough to support a geometry similar to that of **5c**.

Compound **6** is isolated as a binuclear compound with Rh(I) metal centers in a two-legged piano-stool geometry presumably because it is more stable in that geometry than as a complex comprised of a series of six-membered rings with cis-phosphine cis-ether geometry at its Rh(I) metal centers. Although ligand **1b** is very similar to ligand **3b** (Chart 1), a compound with η^6 -arene two-legged piano-stool geometry about each Rh(I) metal center (**7**, Chart 2) is the only product isolated. Most notably, a cis-phosphine cis-ether Rh(I) complex analogous to **5a** is never observed. Explanations for this observation include the following: (1) the 1,4-benzene-substituted ring of **3b** is less electron rich than the 1,4-durene-substituted ring of **1b**, which results in the donation of less electron density to the attached O atoms, making the ether moieties of **7** worse ligands for Rh(I) than the ether moieties of **5b**, and (2) the methyl groups on the durenyl moieties of **1b** offer increased stabilization through van der Waals interactions when they are in close proximity to one another, as they are in **5a** (Figure 1). Similar arguments apply for why compound **8** forms rather than a condensed structure analogous to **5a**.

Even though compounds **6–8** are isolated with bisphosphine η^6 -arene piano-stool geometries about their Rh(I) metal centers similar to **5b**, it is likely that cis-phosphine cis-ether complexes analogous to **5a** are the first products formed, as they are the only ones with the appropriate type of metal binding to direct the formation of the binuclear metal species. Indeed, if the ligands were to bind to one metal center such that the phosphorus and the arene were bound to a Rh(I) atom as in the halves of **5b**, it is difficult to rationalize why mononuclear Rh(I) products such as **5c** do not form to some extent. Therefore, we believe that the cis-phosphine cis-ether structures such as **5a** are the critical

intermediates and structures that make the weak-link approach a viable one for preparing binuclear macrocycles.

The Rh(I)– η^6 -arene and the Rh(I)– η^1 -ether bonds are both stable enough to target **5a**, **6**, **7**, and **8** as high-yield condensed structures. Importantly, both the η^6 -arene–Rh(I) of **5b**, **6**, **7**, and **8** and the η^1 -ether–Rh(I) bonds of **5a** function as weak links for these structures. These bonds are broken by a variety of incoming ligands, resulting in the desired large macrocyclic ring structures in quantitative yields (Scheme 3 and Chart 3).

The first small molecule used to break the weak links of a condensed macrocycle was CO. There are numerous examples in the literature of CO displacing both ether and arene groups bound to Rh(I), and Rh(I) bisphosphine tris-CO compounds are also well-known.^{37,39,41,53} In all cases, exposure of a CH_2Cl_2 solution of condensed macrocycle **5a** or **5b**, **7**, and **8** to CO (1 atm) resulted in the quantitative formation of large homobimetallic macrocyclic ring structures **9**, **10**, and **11**, respectively (Scheme 3 and Chart 3). In this study the sizes of the rings varied from 26 to 34 members, demonstrating one example of synthetic tailorability accessible through this method. By switching to a ligand with a larger aromatic cleft (phenyl vs biphenyl), one can synthesize a macrocyclic structure that is both larger and possesses a more hydrophobic pocket. This tailorability will be important for using these structures as receptor sites for host–guest type chemistry. The relative ease by which one can fine-tune a host macrocycle structure will allow one to easily target the best possible fit for a guest or analyte molecule of interest.

Many metallomacrocycles are prepared by using all of their metals' coordination sites to direct the formation of a structure and hold it together, a strategy that prevents simple ligand substitution reactions at the metal centers.¹³ Macrocycles synthesized via the weak-link approach have several coordination sites that are capable of ligand substitution reactions, allowing for increased ability to control the properties of a macrocycle. This has been demonstrated by the conversion of the trigonal bipyramidal hexa-CO adducts **9–11** to the square-planar bis-CO bis- CH_3CN adducts **12**, **14**, and **15** (Scheme 4). The bis-CO bis- CH_3CN adducts can be synthesized through two routes: (1) by converting a condensed macrocycle to a hexa-CO adduct followed by addition of CH_3CN , or (2) addition of CH_3CN to a condensed macrocycle followed by exposure to CO. This facile ligand substitution makes these compounds attractive candidates for catalysis and as building blocks for more complex three-dimensional structures (e.g., molecular cylinders).²³

Most inorganic macrocycles are limited to using cage effects to sequester molecules via weak interactions (van der Waals or hydrogen bonding). Macrocycles synthesized via the weak-link approach have the demonstrated ability to undergo ligand substitution reactions while maintaining the macrocycle structure. Therefore, the metals in these structures can be used to direct the binding and orientation of molecules within their cavities. We have demonstrated how one can take advantage of this reactivity in proof-of-concept sequestration studies by binding the bifunctional aromatic molecules 1,4-dicyanobenzene and 1,4-phenylenediisocyanide (Scheme

5). The binding of bifunctional aromatic molecules leads to three-tiered structures where the two aromatic groups in the skeleton of the macrocycle line up in a parallel-planar fashion with the sequestered aromatic groups spanning the cavities. The distances between the aromatic groups that are part of the macrocyclic cavity and the sequestered aromatic molecule lead to the conclusion that the binding of these bifunctional aromatics is completely a metal-driven event; indeed, the durenyl moieties in the skeleton of the macrocycle **17** reside beyond the range (4.24 Å) of any π - π stacking interactions that might further stabilize the structure.

Conclusions

We have reported a new and versatile synthetic approach for preparing homobimetallic macrocycles from flexible ligands. By targeting intermediate condensed structures, we have synthesized these macrocycles in exceptionally high yields, overcoming the entropic penalties that normally result in low yields and undesirable oligomeric and polymeric byproducts. It has been demonstrated that this strategy is widely applicable to a variety of ligand types, allowing one to synthesize macrocycles that differ in size, hydrophobicity of macrocycle cavity, and electronic and steric environment around their component metal centers. Furthermore, it has been demonstrated that these macrocycles, and specifically the coordinatively labile metal centers within them, are capable of guiding the sequestration of bifunctional aromatic molecules.

The importance of this new approach depends on its generality toward a number of ligand and metal types. Significantly, concepts presented in this paper should be easily expanded to a variety of ligand types and transition metals. Further research aimed at expanding these methods to other transition metals, building more sophisticated architectures, and developing these structures for sensor and catalytic purposes are underway.

Acknowledgment. C.A.M. acknowledges the Georgia Institute of Technology Molecular Design Institute under ONR Contract No. N-00014-95-1-1116, NSF (CHE-9625391), and PRF (30759-AC3) for support of this research. The University of Delaware acknowledges the National Science Foundations for their support of the purchase of the CCD-based diffractometer (CHE-9628768).

Supporting Information Available: Detailed X-ray structural data including a summary of crystallographic parameters, atomic coordinates, bond distances and angles, anisotropic thermal parameters, and H atom coordinates for **5a**, **5c**, **6**, **7**, **9**, **10**, **12**, and **17** along with an NOE difference spectra of **17**. This material is available free of charge via the Internet at <http://pubs.acs.org>. Further details on the crystal structure investigation may be obtained from the Fachinformationszentrum Karlsruhe, D-76344 Eggenstein-Leopoldschafen, Germany (fax (+49)7247-808-666 (Fraue S. Höhler-Schlimm); e-mail crysdata@fiz-karlsruhe.de), on quoting depository numbers CSD-380141 (**5a**) and -380142 (**17**).

OM990585+